Investigation into the Electrospinning of Hyaluronic Acid

A Thesis

Submitted to the Faculty

of

Drexel University

by

Eric Karl Brenner

in partial fulfillment of the

requirements for the degree

of

Master of Science in Materials Science and Engineering

May 2009

Dedications

To my parents.

For your sacrifices I am eternally grateful.

Acknowledgments

First and foremost, I would like to thank my advisor, Dr. Caroline Schauer. Your help and support has been great and I could not have asked for anything better. Secondly, I would like to thank Jessica Schiffman. I would not have been able to do this without you. Thank you so much for all the time you spent, in addition to your own work, helping in the analysis and characterization of my samples. Also, thank you for all the expertise and guidance in the electrospinning process. You were wonderful to work with. Additionally I'd like to thank all the members of the Natural Polymers and Photonics Lab, including Keith Fahnestock, Aldo DiPrato, Ebony Thompson, Alma Blassengale, Marjorie Austero, and Ari Sagiv. I also extend my gratitude to Amy Peterson from Dr. Palmese's group for her assistance and training on the rheometer as well as Janine Kishbaugh and Dr. Larry Quarino at Cedar Crest College for their assistance with the ATR-FTIR. In addition, I'd like to thank all of my committee members: Dr. Christopher Li, Dr. Michelle Marcolongo, and Dr. Caroline Schauer.

I most definitely would like to thank my parents, who have sacrificed a lot of their time and energy to give me the chance to succeed. I appreciate all that you have done for me, and one day I'll return the favor.

Lastly I'd like to thank my girlfriend Stacie, who I have looked to for strength and support not only throughout my time doing research, but throughout my entire 5 year career at Drexel. You kept me moving forward and were always positive with me. Thank you so much for everything.

Table of Contents

List of Tables

List of Figures

Abstract

Investigation into the Electrospinning of Hyaluronic Acid

Eric Karl Brenner

Caroline Schauer, Ph.D.

Electrospinning has become a popular method for the production of fibrous mats with diameters on the order of a few hundred nanometers. A simple setup has made it a versatile method for the processing of many soluble polymers into such a fibrous state. The fibers formed are capable of being chemically or physically tailored for many applications, most notably tissue engineering and filtration, due to the high surface area to volume ratio that nanofibers exhibit. The process can be adapted to large scale production, which invites much research into developing and completely understanding the process. Some have even considered the process to be an environmentally "green" method of nanomaterial production. [1]

Recently there has been much work involving the use of natural polymers, such as hyaluronic acid (HA) in the form of nanofibrous mats for the previously mentioned applications. Hyaluronic acid is a major glycosaminoglycan found in the extracellular matrix of connective tissue in higher mammals. Therefore, filtration and tissue engineering applications would greatly benefit from the use of this material, especially in nanofiber form. Although, the unique properties of these polymers, including an extremely high solution viscosity at low concentrations as well as their being

polyelectrolytes, have provided for significant barriers to their electrospinnability. Currently carrier polymers, such as poly (ethylene oxide) are required in a blend to successfully produce nanofibers of HA.

This work primarily focused on determining proper solvent systems that allow for the successful production of pure HA nanofibrous mats via electrospinning without the need for blending with other polymers. Specifically, the work involved using strong solvents for HA, either via basic solutions of ammonium hydroxide or aqueous solutions containing DMF and various phosphate salts to change conductivity and rheological properties and allow for successful nanofiber production. Nanofibrous mats of HA were produced in ammonium hydroxide solution as well as in water:DMF solutions containing sodium phosphate, glycerol phosphate and tripolyphosphate.

CHAPTER 1: INTRODUCTION

Today, the majority of plastics used in many industries are petroleum based. While these materials have proven very valuable in a variety of applications, from consumer products to medical technologies, there is growing concern regarding both the origin of the materials, as well as their eventual disposal.

Disposal of such strongly bonded plastic materials in landfills has become a popular topic for discussion in the social and environmental arenas. The high stability of petrochemical based polymers causes the natural breakdown to extend beyond an acceptable time frame, with estimates of over hundreds of years. One reason for this is that there is a lack of micro-organisms that exist today capable of digesting them.[2] While recycling efforts have improved in recent years, the rate at which petro-based plastics are discarded far exceeds that of the recycling rate. While some oil-based plastics are purposely and rightfully used for their long lasting properties and strength, many single use-type materials provide for environmental drawbacks. Therefore, much research has focused on developing methods for converting waste plastics into reusable products, such as gasoline and oil. Pyrolysis, hydrogenation, and gasification are some of the most popular methods for converting organic wastes into usable fuels.[3, 4] Though, the energy requirements for these processes may also outweigh the benefits.

As an alternative, there has been much work to derive and develop highly biodegradable, single use materials from natural sources. Natural polysaccharides, or biopolymers, fit this description. The increased research into natural polysaccharides,

including chitin, its derivative chitosan, alginate and hyaluronic acid (HA) has uncovered vast opportunities in terms of applications. Their increased biocompatibility, great abundance in nature and tremendous chemical properties make them suitable for many applications, including single-use. Among many which will be discussed, tissue engineering, air and water filtration, drug delivery and the food industry are some of the areas in which natural polymers have the potential to become the leading materials of choice. More specifically, their use in the form of nanofibrous mats generated by the process of electrospinning is of great interest.

Before trying to utilize the process itself, it is important to understand the structure and properties of the molecules themselves as these greatly affect their electrospinnability.

1.1 POLYSACCHARIDE STRUCTURE

Many of the properties exhibited by natural polysaccharides result from their chemical and physical composition. Generally speaking, polysaccharides are composed of the same building blocks, although diversity within the structure provides for different properties among molecules.

Polysaccharides form a physical structural hierarchy, much like a similar group of biological materials, proteins. The monosaccharide and its chemical composition is the primary structure. The monosaccharide building blocks are composed of typically 4 or 5 carbon atoms arranged in a cyclic ring structure, termed pyranose and furanose, respectively. [5] Functional groups bonded to the main ring structures give rise to

variable properties among different molecules. These include viscosity and charge differences as well as differences in bonding affinities to external atoms and molecules.[6] When two monosaccharide units are bonded together, they form a disaccharide. The bonds that form between the units are called glycosidic bonds as a functional group tends to bind the two units together.[5] Analogous to the monomer in polymer science, the disaccharide is the repeating unit of the polysaccharide. Repeat units arrange themselves locally and connect to form a periodic chain, also known as the secondary structure.[7] Figure 1 shows several possible secondary structures. Chains can be arranged and composed of the same disaccharide (linear) or can be composed of 2 disaccharides that alternate (alternating repeat), among others also shown.

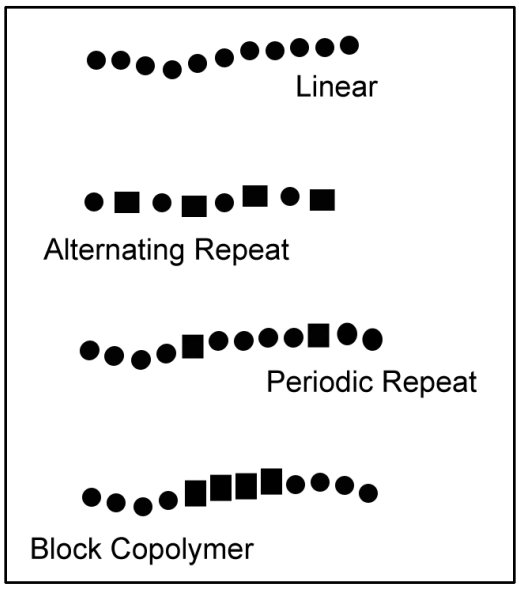

Figure 1: Several Common Polysaccharide Secondary Structures

The chains can then take several conformations, although the packing of the structure is not quite as tight as with proteins. This is termed the tertiary structure. Rotational freedom of the glycosidic bonds allows for such changes in conformation.

Although, there exist many factors that may limit the overall degree of freedom, including steric hindrance and electrostatic repulsions. [7] Finally, the quaternary structure describes the potential assembly and interaction of the molecule with another, different molecule, often forming a macromolecule.

As mentioned earlier, the structure and chemical composition of the polysaccharides give rise to variability among properties. A result of their specific structure and composition, natural polysaccharides can be classified into three groups based on their charge. In contrast to many synthetic polymers which are found to be neutral, many natural polysaccharides are considered polyeletrolytes, being either anionically or cationically charged. Additionally, some natural polysaccharides are also neutral.

1.2 NEUTRAL NATURAL POLYSACCHARIDES

1.2.1 CHITIN

Chitin, a high molecular weight linear polymer, is composed of β(1-4) linked 2-amino-2-deoxy-*b*-D-glucose (*N*-acetylglucosamine). Its structure is shown in Figure 2. A structural polysaccharide, chitin is the second most abundant in nature, next to cellulose. It is most commonly derived from the shells of sea crustaceans, such as crab and shrimp.[8] It is also found in squid pens and insects. Much like cellulose, chitin is hydrophobic and is highly insoluble in water and most organic solvents. It is this property which sometimes limits its uses, although the many derivatives of chitin improve upon

this insolubility. Charge neutrality within the molecule is derived from a lack of charged functional groups within the disaccharide repeat unit.

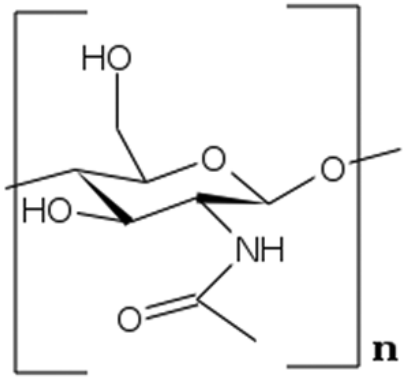

Figure 2: Structure of chitin

Despite its very limited solubility, chitin has been researched extensively for use in several industries, including biomedical, cosmetic, as well as food additives. [9] The ability for chitin to form microcrystalline films is a useful property in food coatings. In edible thin film form, such coatings provide for temperature stability as well as low oxygen permeability.[10] Chitin has been shown to bind metal ions quite strongly due to a high nitrogen content.[8] The chelation properties of chitin to metal ions such as palladium, copper and silver is therefore useful in insecticides, photography, and catalysts among many others applications.[11]

Aside from bulk form, chitosan has also been investigated in fiber form, both on the micro- and nano- scales. Fiber spinning methods have been adapted to produce fibers of chitin. Various solvent systems have been investigated, ranging from halogenated solvents [12] to Amide-LiCl solvents. To date, many of the solvents used to dissolve

chitin are acid based, with some being quite corrosive as well as extremely expensive. This too, has limited the applications for chitin-based fiber structures.

In addition to fiber spinning methods producing micron size fibers, chitin has also been investigated in the electrospinning process. Recent attempts at electrospinning chitin have been successful by Min *et al.* in solvents such as hexafluoroisopropynol (HFIP). [9] Both nano- and micron size fibers of chitin are useful in a variety of applications. Due to the similarity regarding chitin fiber applications with its derivative chitosan, they will be discussed with chitosan in order to avoid redundancy.

1.3 CATIONIC NATURAL POLYSACCHARIDES

1.3.1 CHITOSAN

Chitosan, much like chitin, is a common structural polysaccharide found in the exoskeletons of many crustaceans. Chemically, chitosan is the *N*-deacetylated form of chitin (Figure 3). Considered a linear block copolymer, it is composed of β (1-4) linked D-glucosamine residues. Within that repeating structure, there are randomly inserted *N*-acetyl-glucosamine groups. Chitosan is considered a semi-crystalline polymer, although the degree of crystallinity depends greatly on the degree of deacetylation. [13] Deacetylation involves the removal of acetyl groups from the structure of chitin. Acetylated amine groups in chitin are converted to primary amines in chitosan. [14] Complete deacetylation is not common, and thus the degree of deacetylation (DD) is a

well known method for characterizing chitosan. Typical commercial DD values range from 60-80%. [15]

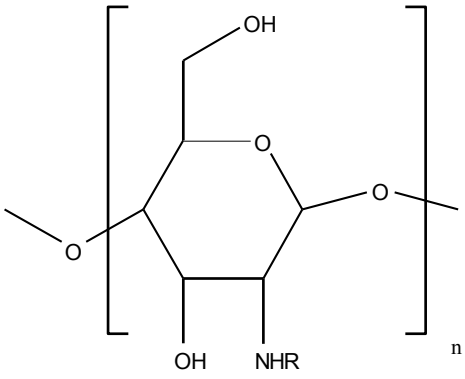

R = H, or acetyl

Figure 3: Structure of Chitosan

The deacetylation process is helpful in overcoming the poor solubility properties of chitin while retaining many of the useful properties associated with polysaccharides. For example, the heavy metal-ion chelation ability is retained. While chitosan is still hydrophobic, it is soluble in dilute acids, such as acetic acid and formic acid.

Additionally, the cationic nature of chitosan is derived from the existence of primary amine groups. Charged polymers, or polyelectrolytes, are interesting as they behave much differently than neutral polymers. The charged species along the polymer chain give rise to electrostatic repulsions when in solution. These charges are often balanced by counter ions. Therefore, with charge carriers and counter ions available, polyelectrolyte solutions also exhibit higher electrical conductivities than their neutral counterparts. [16] Charge density is consequently greater in these solutions as well.

Chitosan is typically crosslinked using a variety of chemicals to control reactivity, and to increase the overall stability of the material. These include glutaraldehyde [17], hexamethylene 1,6-di(aminocarboxysulfonate) (HDACS) [18] and epichlorohydrin [19], among many others. Crosslinking via glutaraldehyde takes place by two main methods. Michael-type leads to the formation of carbonyl groups by terminal aldehydes, while Schiff-based functionality leads to imine formation. [17] In general, crosslinking via the amine groups has proven more effective as side reactions with alcohols or water are dramatically slower than the crosslinking rate reaction. [18]

With many unique properties, there exist a number of applications for chitosan as well as its acetylated parent molecule, chitin, in the bulk form. Fungicidal properties of both chitin and chitosan have lead to uses in cosmetic products such as creams and lotions. [11] Chitosan has also been investigated in hydrogels for drug delivery. Hydrogels are capable of absorbing a great amount of water, and chitosan-based hydrogels regulate their water uptake based on the pH of the surrounding environment. [11] Additionally, the extent of crosslinking in the chitosan also affects the sensitivity of swelling to pH.[20] This influence on swelling has a subsequent effect on drug diffusion rate, creating possibilities for controlled drug delivery applications, especially in areas of extreme pH changes, such as the stomach. Additionally, as chitosan is degraded *in vivo* via enzymatic hydrolysis, its biodegradability is of paramount importance.[13]

In addition to biomedically related applications, the chelation properties of chitosan are also important in filtration applications. Chitosan membranes have been shown by Silva *et al.* to selectively permeate various solutes depending on structural similarity and extent of chitosan crosslinking. [21] This selectivity also extends to heavy-metal cations.

The mechanism for such chelation properties is by electrostatic attraction between the ion and the free amine groups on the chitosan molecule. [22]

Successful production of pure chitosan nanofibers by electrospinning has been carried out in various solvent systems, including acetic acid and trifluoroacetic acid. [17, 22-25] This typically results in non-woven mats produced of fibers on the order of hundreds of nanometers. Nanofibers and electrospinning will be discussed in detail in subsequent sections. The advantage of creating a fibrous form of chitosan is that nanofibers exhibit a greatly increased surface area to volume ratio. Many of the applications in which chitosan has been used can be improved via its use in nanofiber form.

In terms of biomedical uses, chitosan and chitosan-based nanofibers exhibit antibacterial and wound-healing capabilities and therefore have been explored for use as sutures and as wound-dressings. [14, 23, 26] The nanofibrous structure promotes skin growth, and additionally, wound healing can be accompanied by doping the fibers with a drug to be delivered in a controlled manner.[27] Additionally, non-woven nanofibrous mats composed of materials including chitosan are ideal candidates for use as tissue engineering scaffolds. [27, 28] Duan *et al.* have blended chitosan with other polymers, PLGA and PVA in an electrospun fibrous membrane and observed degradation and compatibility properties *in vitro*. [29] Acting as a mechanical support, a chitosan based fibrous structure can aid in the regeneration of tissue and the proliferation of cells.

Filtration uses can also be improved by the high surface area properties of nanofibers in general. Desai *et al.* have shown that blended electrospun fibrous mats of chitosan and

poly(ethylene oxide) are extremely capable of acting as effective air and water filtration materials.[22] These mats are proficient at chelating a wide variety of solutes, including metal ions and microbes. High-end, single-use air filtration devices can be made much more environmentally friendly by utilizing devices made from chitosan-based materials.

1.4 ANIONIC NATURAL POLYSACCHARIDES

1.4.1 ALGINATE

Alginate is a negatively charged natural polysaccharide which is commonly derived from brown seaweed. Its structure is given in Figure 4. The structure of alginate is considered to be that of a linear block co-polymer, as the chain consists of varying fractions of the two monomers, 1,4-linked β-D-Mannuronic acid (M) and α-L- Guluronic acid (G) (also referred to as Mannuronate and Guluronate, respectively).

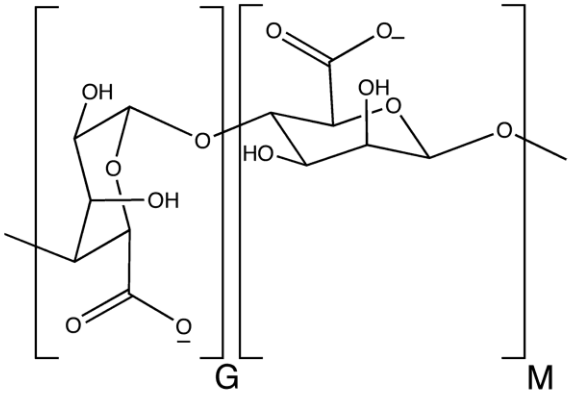

Figure 4: Structure of Alginate showing both Mannuronic Acid (M) and Guluronic Acid (G) monomers

Extraction of alginate from different species of brown seaweed leads to varying G and M content and the variability in the G-to-M ratio subsequently controls the resulting physical properties. Additionally, there are effectively three blocks which can appear along the chain of the alginate molecule. These include MM, GG and MG blocks. Similarly, the properties of various alginates can also depend on the relative proportions of these blocks found along the chain. [30] Such diversity among alginates makes it promising for use as an industrial, petro-based polymer replacement. [31]

Alginate gains negative charge from the carboxyl groups located on the ring structure of both the M and G monomers. Unlike chitosan, alginate is readily soluble in water. Although, they are similar in the fact that once in solution they exhibit a much higher electrical conductivity than other, neutral polymers. The water solubility of alginate makes processing more user friendly, both in terms of applications and crosslinking.

Metal-ion adsorption of alginate leads to a well observed gelation behavior.[32-35] This is commonly seen upon the addition of divalent calcium ions. Chelation of the Ca^{+2} ions leads to what is commonly referred to as an "egg-box" structure (Figure 5) and a Ca-Alginate gel is formed. The Ca^{+2} ion effectively acts as a chemical crosslinking bridge between the guluronate units. Such coordination is favored in the G-units rather than the M-units as a result of the axial orientation of the O-1 linked oxygen in guluronate versus equatorial positioning in mannuronate. [36] Thus, gelling behavior is more prevalent in high-G alginates. Alginate gels formed this way exhibit high stability and limited water uptake, although this can be altered by contact with other ionic compounds, such as phosphates, where ion exchange becomes a dominant reaction.[32] This gelling behavior is a common method for the chemical crosslinking of alginate.

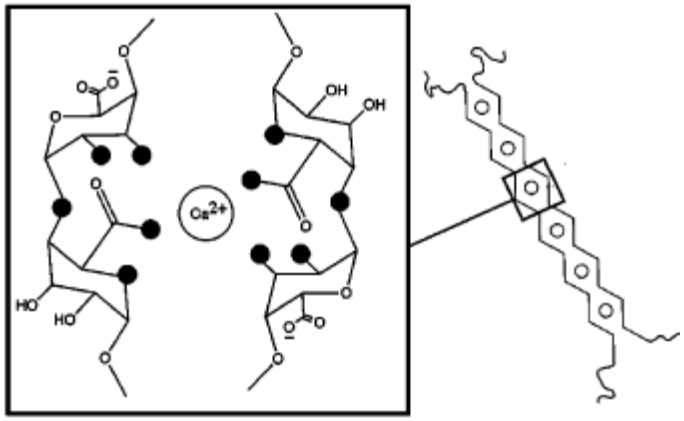

Figure 5: "Eggbox" structure formed by crosslinking with divalent Calcium ions (Reproduced from [37])

Alginates, like chitosan, have many potential uses in bulk form. Due to biocompatibility and protein release properties of alginate matrices, there has been extensive interest in drug delivery applications.[38] The pH sensitivity and the stability of alginate based beads and emulsion beads have been developed for controlled drug delivery systems.[39] Chitosan /calcium-alginate beads have also been developed specifically for the oral delivery of insulin. [40] While many alginate gels formed by the chelation of calcium ions have been used for wound dressings and tissue regeneration, the potential risk of high calcium ion concentration causing toxic foreign body reaction has lead to new crosslinking methods, such as covalent methods using ethylenediamine.[41]

With metal ion chelation properties similar to chitosan, alginate thin films have also been investigated for use as sensing materials. Changes in refractive index or

physical thickness changes in the films as a result of such binding interactions allow for detection and recovery of toxic ionic species in many aqueous environments. [37]

1.4.2 HYALURONIC ACID

Hyaluronan, or hyaluronic acid (HA,) is a major glycosaminoglycan, which is found in the extracellular matrix of many soft connective tissues in higher animals. Common concentration levels in various tissues and fluids given in Table 1 provide an overview of the abundance of this natural polymer. HA has been recognized in a number of physiological roles, including cell differentiation and mitosis. Additionally, they have been found to be the primary target of many hyaluronan based receptor proteins. [42]

Tissue or fluid	Concentration, mg/l
Rooster comb	7500
Human umbilical cord	4100
Human synovial fluid	1420–3600
Bovine nasal cartilage	1200
Human vitreous body	140–338
Human dermis	200
Rabbit brain	65
Rabbit muscle	27
Human thoracic lymph	8.5–18
Human urine	0.1–0.5
Human serum	0.01–0.1

Table 1: Concentrations of Hyaluronic Acid in various tissues and fluids. Reproduced from [42]

A linear polysaccharide HA is composed of repeating disaccharide units of β-1,4-D-glucuronic acid and β-1,3-*N*-acetyl-D-glucosamine. The structure is given in Figure 6. Like alginate, HA is a highly viscous, negatively charged, natural polysaccharide that is

easily dissolved in water. The molecules are quite similar, with the major functional groups being hydroxyl and carboxyl groups. It can be crosslinked using similar crosslinking agents, such as glutaraldehyde and carbodiimides. [43, 44] Recently there has been success in crosslinking HA using divinyl sulfone, which requires alkaline environment for the reaction to take place. [45-47]

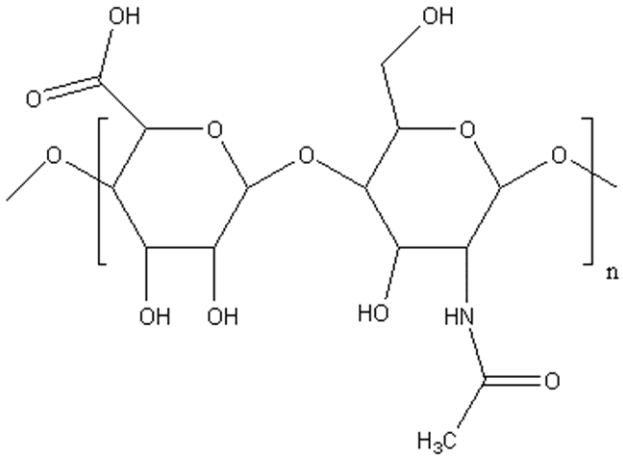

Figure 6: Structure of Hyaluronic Acid containing glucuronic acid (left) and *N*-acetylglucosamine (right)

The negative charge and rheological properties allow for a range of biomedical applications in the bulk form. Since HA is already a major component of the extracellular matrix, it has been widely investigated as scaffolding material for cartilage tissue engineering in the treatment of arthritis. [48-51] Similar methods for tissue repair have used HA as a carrier for cells. Synthetic matrices and materials that are HA-based allow for the mimicking of the HA-rich embryonic stage, and can therefore allow for significantly more effective cell development and ultimately, tissue repair.[52]

While HA has excellent biocompatibility, the anionic and hydrophilic properties of many HA materials do not favor the direct attachment of cells. [49] This has led researchers into finding ways to improve such properties. Several methods have been investigated, including combining HA materials with other materials which are more cell-friendly, such as collagen. Alternatively, creating a three dimensional or a porous scaffold can help for the proliferation of cells. Such scaffolds can be produced by electrospinning.[49]

CHAPTER 2: BACKGROUND

2.1 ELECTROSPINNING PROCESS

2.1.1 NANOFIBERS

Electrospinning is currently the best method for producing continuous, non woven mats of nanofibrous material. Nanofibers produced by this method have diameters that range from sub-micron to the nanometer scale. Typically, the diameters are roughly a few hundreds of nanometers. Polymer materials that can be produced in this form have a number of key properties, which can be utilized to improve their applications.

The nanometer scale of the fibers contained within the mat allows for an extremely high surface area to volume ratio. This ratio can be as large as 1000 times higher than those micron-size fibers produced by traditional fiber spinning methods. [53] It is this property which attracts the most attention in terms of research and ultimately, final applications.

Additional properties include excellent surface modification. Nanofibrous mats can be tailored to incorporate numerous functionalities. To add, mechanical properties, most notably the tensile strength, are vastly improved in the transition from micron to nanofibers, and can help to stabilize the fibrous mats in various applications.[53] Additionally, the increased surface area can result in less overall material needed in terms of applications.

Greiner *et al.* provide an example which conveys the versatility and efficiency of producing nanofibers of any given material versus the bulk. [27] Fibers of 10 µm produced from 1 kg of polyethylene can extend 13 km. In contrast, nanofibers of diameter 100 nm produced from the same mass of polyethylene can produce fibers which extend over 130,000 km. The specific surface area of the nano-scale fibers is also measured at roughly 100 times that of the micron–scale fibers.[27]

2.1.2 SETUP

The electrospinning setup includes several parts. The basic layout is shown in Figure 7. The polymer of choice is first put into solution and then loaded into a syringe. The syringe is connected to a high voltage power supply via the capillary tip. The needle tip can be of various diameters which commonly depends on the rheological properties of the polymer solution. The entire syringe-needle combination is connected to a feeding pump, which forces the solution through the syringe at a fixed rate. The pump is typically calibrated according to the needle size used as to provide accurate feed rates as defined by the user.

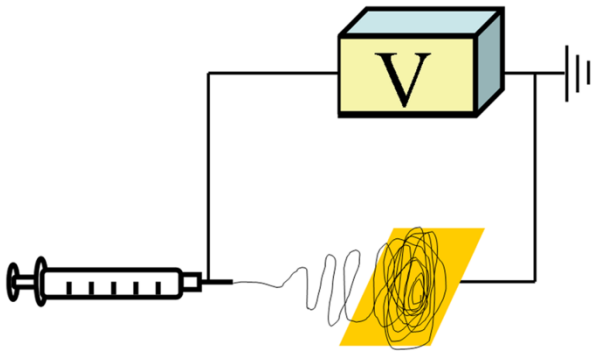

Figure 7: Simplified schematic of electrospinning process

As the capillary tip acts an electrode, a conductive collector plate often placed anywhere between 3 and 30 cm from the tip serves as the grounded counter electrode. The power supply provides an applied DC voltage and a subsequently produces an electric field on the order of 100-500 kV m^{-1}. The applied voltage is commonly provided at amperages ranging from a few hundred nanoamperes to microamperes. [27] This applied field induces charges interactions within the polymer solution which contribute to fiber formation. The exact mechanism will be discussed later.

2.1.3 TAYLOR CONE

As the solution is forced through the needle, a droplet forms on the end of the capillary tip. The applied electric field electrifies this droplet, inducing charges which are spread evenly across the surface of the droplet. The droplet then experiences two forces. Li and Xia explain that the droplet will experience electrostatic repulsions between the induced surface charges as well as Coulombic forces that are present due to the external electric field. [54] The repulsive interactions between charges creates a force directly perpendicular to that of the surface charge [55]. The shape of the droplet is altered as the charges accumulate and it takes a conical form at the tip of the needle. This is typically referred to as a Taylor Cone [54, 56]. Once the applied electric field exceeds a certain threshold, typically the surface tension of the solution, the Taylor Cone is elongated and forced from the tip as a liquid jet, as shown in Figure 8.

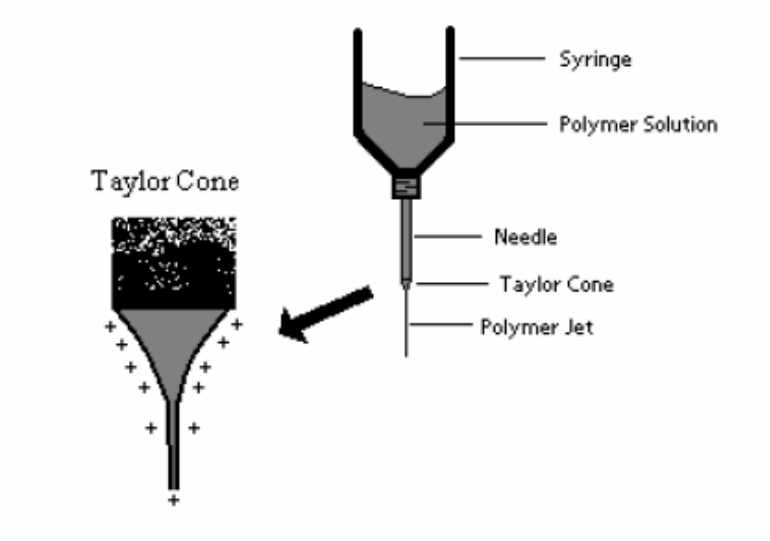

Figure 8: Accumulation of charges and formation of the Taylor Cone. Reproduced from [56]

Yarin *et al.* have recently shown that the altered droplet at the end of the capillary does not necessarily take the form of a Taylor cone, but rather a different shape. They have shown, both theoretically and experimentally, that a liquid droplet, upon application of an electric field, forms a conical shape with a half angle of 33.5°, which is much smaller than the requirement of 49.3° for a Taylor cone [57]. Thus, the conical shape is essentially sharper than that of the typical Taylor cone. The effect of various shapes of the droplet prior to jet initiation have been correlated with various instabilities within the liquid jet [58].

2.1.4 BENDING INSTABILITY AND FIBER FORMATION

In general, the electrospinning process can be attributed to a number of instabilities in the polymer solution. Instabilities formed in the electrified solution, especially in the liquid jet, play a critical role in altering the path of the jet and ultimately on fiber formation.

Overall, the electrified jet produced is subject to constant elongation and whipping to the point of fiber formation on the collector plate. Combined with the evaporation of the solvent used, this allows for the formation of ultra-thin fibers[54]. But the alteration of the jet into a circular path known as the conical envelope, as shown in Figure 9, can be attributed to what is commonly known as bending instability [54, 55, 57, 59-61].

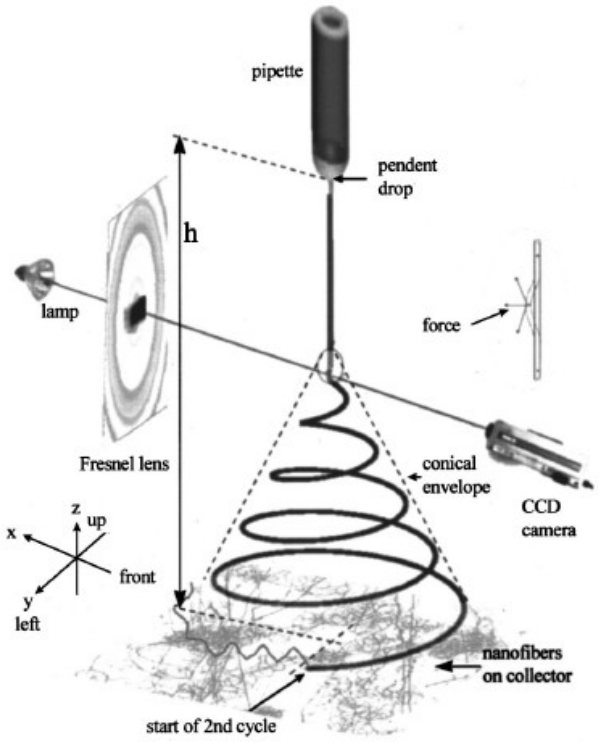

Figure 9: Electrospinning Process showing electrically induced bending instability and formation of the conical envelope. Reproduced from [59]

Reneker *et al.* showed that the jet initially flows away from the droplet in a straight line as a result of the longitudinal stresses from the electric field on the carried charge [59]. As mentioned earlier, the diameter of the fiber decreases due to elongation and solvent evaporation. A smaller jet diameter thus creates an increased surface charge

density. [55] Adjacent charges along the jet then begin to repel, creating a lateral instability. The resulting bending instability contributes to the looping motion and further stretching of the jet [59]. The jet is eventually freed of solvent and a solidified polymer fiber results. The fibers are then collected on the plate as a non-woven, randomly oriented mat. [54]

2.2 SOLUTION PARAMETERS

There are many factors that affect both fiber diameter as well as overall nanofiber production. Firstly, the chosen polymer solution has many characteristics and properties that may or may not be suitable for electrospinning. These include concentration, zero shear rate viscosity, elongational viscosity, charge density, conductivity, and relaxation time, among others.

Solution concentration is critical for the formation of continuous and consistent fibers in the electrospinning process. If a polymer solution concentration is too low, there won't exist enough chain entanglements for electrospinning and the solution will lack viscosity. Conversely, too high of a concentration will create an extremely viscous solution and the applied electric field will not be strong enough to overcome this and a polymer jet will not be formed.

Zong *et al.* have shown that concentration and corresponding viscosity of a solution can also have drastic effects on fiber morphology.[62] More specifically, beaded fibers were produced and observed from poly(D,L-lactic acid) (PDLA) solutions at roughly 25%. Figure 10 exemplifies such a structure which is commonly referred to as

"pearls on a string." Upon an increase in polymer concentration to 30% and thus an increase in viscosity, the distance between beads decreased and smooth, uniform fibers were observed. Fiber diameter also increased with viscosity. A possible reason for such an observation is that at low concentrations, fibers that reach the target are still wet while higher concentrated solutions produce fibers which solidify upon reaching the target. Wet fibers that reach the target undergo significant relaxation due to their viscoelastic nature. [62] Therefore it is widely reported that higher concentrations result in larger fiber diameters. [27, 53, 54, 60]

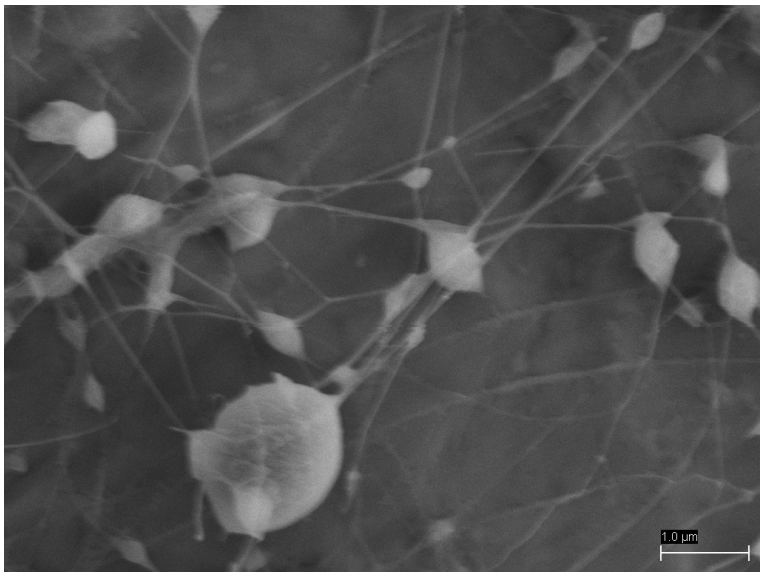

Figure 10: Beaded fibers from blended solution of 2:1 Alginate:PEO in H_2O

The mathematical dependence of fiber diameter on concentration can be summarized by a dimensionless parameter called the Berry number (*Be*). The Berry number is defined by:

$$Be = [\eta]^{*}C \tag{1}$$

where [η] is the intrinsic viscosity of the polymer and C is the concentration of the polymer solution. [63, 64] The intrinsic viscosity can be defined as the ratio between specific viscosity and concentration at infinite dilution. This relationship is designed to show not only the relationship between polymer concentration and fiber diameter, but also the effect that polymer conformation has on the same parameter. More specifically, the Berry number is a measure of the extent of chain entanglements in a polymer solution. [63] The range of the Berry number values are considered to be dependent on the polymer being electrospun, and thus an important parameter in determining the spinnability of a chosen polymer system. [65]

Ko *et al.* have shown that for various values of Be for a given polymer, the resulting fiber diameter and morphology are very different. [66] For Be values less than one, the polymer solution is very dilute, resulting in a minimal number of polymer chains becoming entangled. This effectively inhibits electrospinning of continuous fibers. Conversely, for Be values greater than one, the polymer chain conformation exhibits many entanglements resulting from higher concentrations and consequently, a higher viscosity. A Berry number of greater than one is most favorable for the formation of fibers in electrospinning. [66] As a higher concentration has proven to result in larger fibers, fiber diameter has been shown to increase with Berry number. The effect is shown in Table 2.

	Region I	Region II	Region III	Region IV
Berry Number	Be < 1	1 < Be < 2.7	2.7 < Be < 3.6	Be > 3.6
Polymer Chain Conformation in Solution				
Fiber Morphology	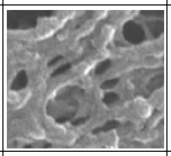	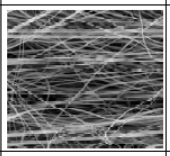	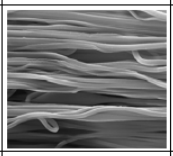	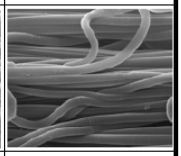
Average Fiber Diameter (nm)	(Only droplets formed)	~ 100 – 500	~ 1700 - 2800	~ 2500 - 3000

Table 2: Influence of Berry number on fiber formation and diameter, Reproduced from [66]

The initial elongational viscosity is also considered a strong factor in affecting fiber diameter. [67] This parameter describes the point where the polymer solution is stretched at the tip of the Taylor cone and formation of the jet begins. Simply, a higher elongational viscosity induces a stronger stretching, resulting in fibers of finer diameter. Thompson *et al.* also state, though, that this parameter cannot be considered an independent parameter, despite its role as a critical factor in affecting final fiber diameter [67] (See Figure 11). The reason for this is that higher elongational viscosities can also be a function of applied voltage, which is considered a user-controlled setup parameter.

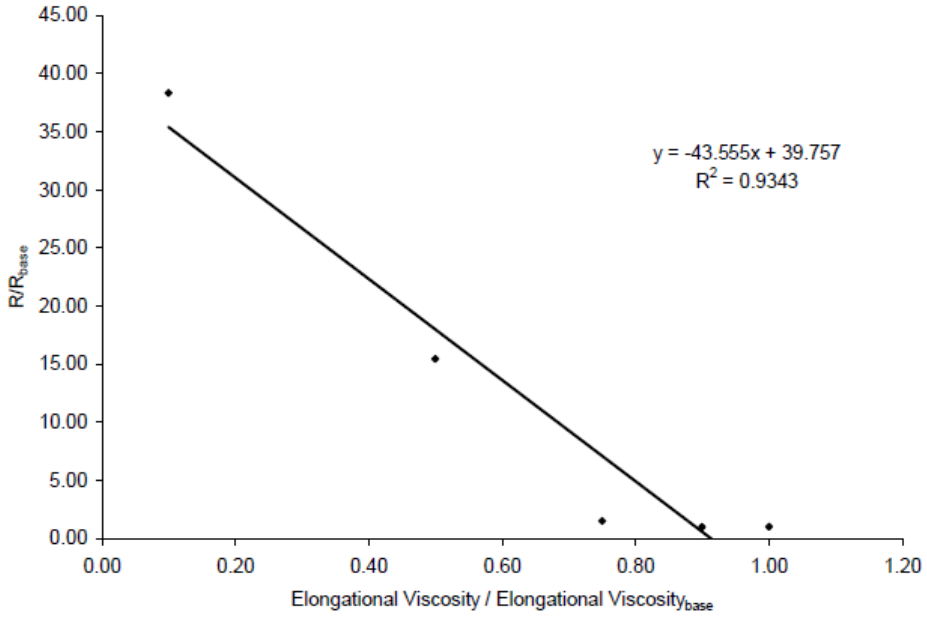

Figure 11: Correlation between Elongational Viscosity and Fiber Radius. Reproduced from [13].

Thompson also concluded via a theoretical model that relaxation time is another critical parameter affecting nanofiber morphology.[67] This is in accordance with Zong's theory as mentioned earlier. [62] In polymers, relaxation time describes the amount of time needed for chains to transition from a high energy conformation to a low energy conformation. [68] By comparing the results of their model to reported relaxation times of polymer solutions[69, 70], they observed a trend which moderately describes increasing fiber diameter with increased relaxation time.

The conductivity of the chosen polymer solution can also determine both electrospinnability and fiber morphology. Conductivity of a solution is dependent on the

number of ionic charge carriers present. A higher conductivity would imply a higher number of charge carriers, and thus a higher charge density, especially on the surface of the Taylor Cone. An increased charge density ultimately increases the strength of the applied electric field as more charge carriers, including those induced by the applied field, are available to be pulled into the resulting jet. Increasing the conductivity of a solution can also help to eliminate the formation of beaded fibers. [27] An increase in conductivity can be completed in several ways. The most common method is the addition of ionic salts to the chosen polymer solution.[71] Additionally, the use of basic and/or acidic solvents, such as aqueous NaOH, can also drastically increase solution conductivity. Conductivities of polymer solutions can range from micro- to millisiemens per centimeter.[72]

2.3 ELECTROSPINNING PARAMETERS

The process of electrospinning contains many variables, which may be adjusted to affect the size and morphology of the fibers. Similar to the solution parameters described above, the particular settings used are also a strong function of the polymer and solution being used. These variables include applied voltage, needle to collector distance and solution feed rate. Additionally, variations to the traditional setup can also help to control fiber morphology and topology.

High viscosity solutions increase the difficulty to electrospin. Adjustments are often necessary to produce fibers. Viscous solutions require a larger electrode separation, or the distance between the needle tip and the collector plate. As a result, in order to

maintain the same electric field strength, the applied voltage must then be increased.[27] The opposite is also true for more dilute and less viscous solutions. Increased electrode distance creates a larger atmospheric gap, most often air, which allows for increased solvent evaporation.

Correlations exist that show the increased prevalence of beaded fibers when an increased voltage is used. [54, 69, 73] The reason for this is that an increased voltage alters the shape of the solution drop at the end of the needle. The new shape inhibits the stability of the formed jet, thus increasing the amount of beads.[73] The overall strength of the electric field is also believed to have an effect on the formation of beaded fibers. Decreasing the field strength has shown to decrease the number of beaded fibers.[61] Therefore, highly viscous solutions are more prone to producing beaded fibers due to higher voltages and field strengths. There may exist a tradeoff between electrospinnability and ideal fiber morphology.

Conflicting opinions exist in the literature regarding the effect of voltage on fiber diameter. [54] Demir *et al.* state that an increased amount of fluid in the polymer jet as a result of higher applied voltages created polyurethane fibers with increased diameters. [74] Conversely, Yuan *et al.* state that increased voltages lead to fibers of bisphenol-A polysulfone with smaller diameters.[75]

Solution feed rate is well-known to directly affect fiber diameter. Increasing feed rates leads to thicker fibers.[28, 54, 62] Consequently, this can be compared to the effect of applied voltage. Demir states that higher voltages can pull the polymer solution from the needle tip faster than it is delivered by the feed rate, therefore altering the conical

bead and the overall stability of the jet. [74] Thus there exists a recognized, but vaguely understood correlation between feed rate and voltage and their effect on both bead formation and fiber diameter.

2.4 CONTROLLING FIBER TOPOLOGY

Often it may be beneficial to modify the basic electrospinning system to allow for specifically controlled fiber morphologies. This includes orientation of produced fibers, as well as producing hollow fibers, among many others.

The traditional electrospinning setup uses a stationary, most often flat collector plate on which fibers are deposited. The fibers are not oriented in any particular fashion, but rather collected as a non-woven mat. It is possible, by the use of a rotating cylinder or disc as a collector plate, to align the produced fibers in a particular orientation (See Figure 12). This becomes quite important in any applications involving fiber-based reinforcement. [54] Boland *et al.* have demonstrated this method in the production of aligned poly(glycolic acid) nanofibers. They showed visual alignment of fibers when the PGA solution was deposited onto a cylinder rotating at 1000 rpm.

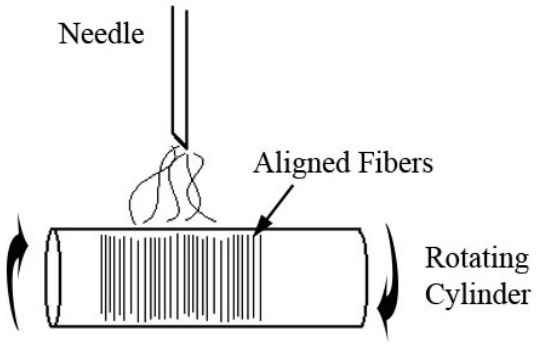

Figure 12: Schematic Showing Electrospinning setup for oriented fiber production

Hollow or tubular nanofibers have also drawn much interest in the literature for the wide variety of potential applications. Such hollow structures can become quite useful in microfluidics, gas storage as well as drug delivery. [54] Li and Xia have produced hollow TiO_2/poly(vinyl pyrrolidone) nanofibers via the setup shown in Figure 13.[76] A coaxial jet was formed between the two immiscible solutions. Once fibers were formed, the interior oil cores were removed by octane, resulting in hollow composite fibers.

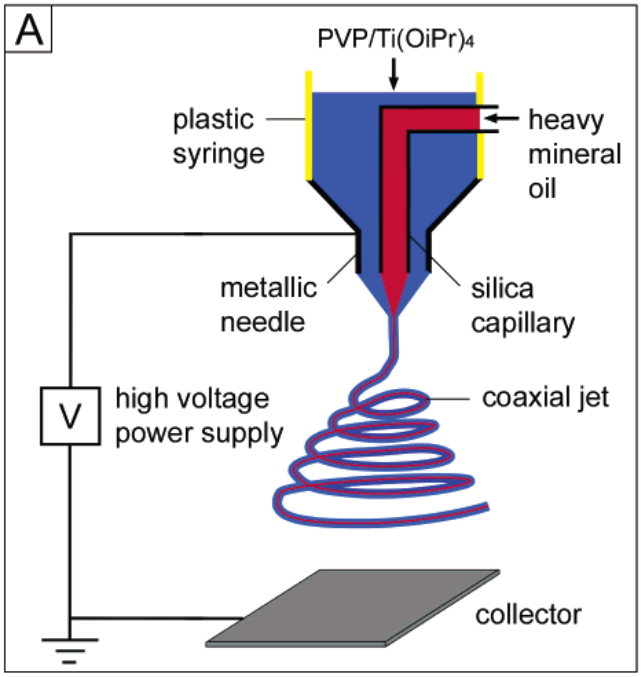

Figure 13: Coaxial Electrospinning Setup for Hollow Nanofiber Production. Reproduced from [76]

2.5 PROBLEMS IN ELECTROSPINNING

It is evident that non woven nanofiber mats can have a distinct affect on a variety of applications. Either by improving existing applications or creating new ones, pure nanofibrous mats from natural polymers are highly desired. But while there has been success with producing nanofibers of pure chitosan, there has been extreme difficulty in electrospinning pure nanofibrous mats of HA and alginate.

Firstly, the extremely viscous solutions that these polymers form at low concentrations impede the processability by electrospinning. While high viscosities make it difficult to pump the solution through the syringe, more importantly they also prohibit the polymer from achieving the proper chain entanglement required for successful electrospinning. The Berry number suggests that a concentration of 2-2.5 times the entanglement concentration is recommended and necessary for successful production of nanofibers.[63, 64] This is easy to obtain using many common synthetic polymers, although trying to obtain a usable solution from many natural polymers is extremely difficult.

To compare, the electrospinning of synthetic polymers such as poly(ethylene oxide) (PEO) and polystyrene has been published using concentrations higher than 20 wt %. [77, 78] At this concentration the polymer is well above the entanglement concentration, as well as within the range suggested by the Berry relationship. Additionally the viscosity of such a solution is well within an acceptable range for processing. For this reason, synthetic polymers like PEO and poly(vinyl alcohol) have been blended with natural polymers such as alginate and HA in order to improve their

electrospinnability.[49, 72, 79-81] Currently, this is the most common method for producing mats of alginate and HA nanofibers.

A major factor contributing to the high viscosity properties is that such natural polymers are charged. The charges along the chain allow for electrostatic repulsions which effectively prohibit the chains from entangling. The flexibility of the chains is hindered and the interaction between them is harder to achieve. The chains act as independent, and extended rigid rods rather than forming an entangled complex.

As a result, there has been extremely limited amount of literature related to the electrospinning of pure nanofibrous mats of alginate or HA. Nie *et al.* have claimed success in producing such pure nanofibrous mats of Alginate using a Glycerol:H_2O solvent system. [82] Similar claims have been made for HA, where various other solvent systems were used, including NaOH:DMF and DMF:H_2O. [50, 83] Lastly, there has been reported success of spinning pure HA solutions using an altered electrospinning setup, termed electroblowing. In the process, heated air is passed over the jet to assist in fiber formation. [84] A major problem with all of these studies, though, is that in each case, except for the modified electroblowing setup, the average fiber diameters of the resulting electrospun mats were much higher than 100 nm, beyond the realm of what is termed a nanofiber. Additionally, the only solvent system in which successful electrospinning could be reproduced by the author was using NaOH:DMF, and thus an aim of this research will be to improve upon these early successes by producing robust, chemically crosslinked mats with fiber diameters less than 100 nm.

There has been success however, in the electrospinning of synthetic anionic polymers, such as poly (acrylic acid) (PAA).[85-87] In addition, the affect of salts (NaCl) on the rheological properties has been evaluated.[88] In the aqueous, dilute regime, the PAA polymer chains exhibit an extended conformation. With the addition of NaCl, the chains appear to shrink and the η_{sp}/c values of such solutions appear significantly lower than those aqueous solutions without salt. While these results provide adequate results to describe the rheological effects in synthetic polyelectrolyte systems, it cannot be directly correlated to natural polyelectrolytes. One reason is that there is a larger abundance of functional side groups in molecules like HA, alginate and chitosan. Secondly, while HA is polyanionic like PAA, the molecule itself is much larger, with a molecular weight sometimes several orders of magnitude higher. Therefore research into salt interactions with HA will also be included.

Overall, the major aim of this research will be to understand and overcome the barrier in producing pure nanofibrous mats of HA. Specifically, the rheological and conductivity properties of various HA solutions will be investigated. It is important to understand why certain solutions allow for electrospinning while others seem to prevent or inhibit the process. By comparing the conductivity and rheological properties of both natural and synthetic polymers which have been electrospun successfully (such as chitosan and PEO) with those unsuccessful solutions of alginate and HA, it may uncover important correlations between the two. More conductive solutions may help to neutralize the electrostatic interactions between the charged chains, and the addition of phosphate salts to the solutions may also help to achieve this result. Neutralization may help to enable or manipulate the entanglement of chains and ultimately, the electrospinning of

their solutions. Also, a higher conductivity implies a higher concentration of charge carriers on the pendant drop which can favor successful electrospinning. Any changes in viscosity as a result of conductivity change can be documented among different solutions. Overall, the results will uncover any correlations which may aid in the production of nanofibrous mats not only from natural polymers, but other materials which may become of interest in the future.

CHAPTER 3: EXPERIMENTAL

3.1 MATERIALS

All materials were used in their as-received condition. The chemicals and reagents used in the experiments, along with manufacturer and grade information is given in a table in Appendix A.

3.2 ELECTROSPINNING

3.2.1 TRIALS

Various solvent systems were prepared utilizing both alginate and HA in an attempt to successfully electrospin pure nanofibrous mats. Tables found in Appendix B and C outline the solution contents and components as well as the electrospinning conditions used. All solutions prepared were mixed using an Arma-Rotator A-1 (Bethesda, MD).

All electrospinning trials were conducted using a bench top setup which resembles a typical electrospinning apparatus, shown in Figure 14. Luer-Lok syringes(5 mL) (Becton Dickinson & Co, Franklin Lakes, NJ) were loaded with the electrospinning solution. Precision glide needles of specific gauge were attached and connected to the positive electrode of a 40kV high voltage power supply (Gamma High Voltage Research, Ormond Beach, Fl). The syringe was placed into an advancement pump (PHD 2000, Harvard Apparatus, Plymouth Meeting, PA) while the negative electrode was connected to a square copper collector plate covered with removable aluminum foil, via alligator clip. The temperature (degrees Celsius) and percent humidity in the laboratory during

electrospinning were monitored by a digital thermohygrometer (Fisher Scientific, Pittsburgh, PA).

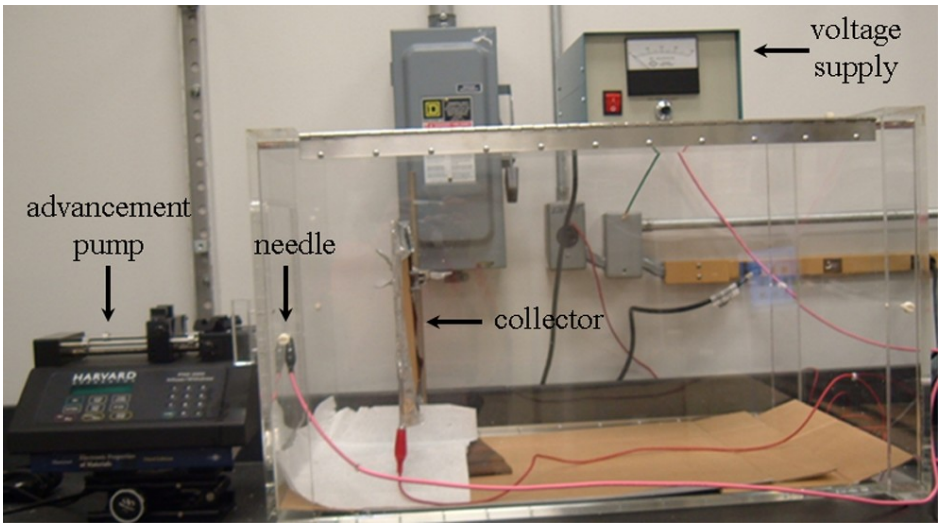

Figure 14: Electrospinning Setup

3.2.2 HA NANOFIBROUS MAT PRODUCTION

Nanofibrous mats of pure HA were obtained using the solvent system outlined by Kim *et al.* [50] A solution of 3 w/v% HA in 4:1 .5M NaOH:DMF was used and studied in subsequent experiments. For electrospinning, a voltage of 10kV was used. The needle to collector plate distance was 5 cm, and the solution feed rate was set to 15 µl/min. Additionally, the solution was pumped through a 21 gauge needle.

Additionally, HA nanofibrous mats were obtained using an ammonium hydroxide solvent system. 1.5 w/v % HA in 2:1 and 1:1 NH_4OH:DMF was used as the electrospinning solution at a voltage of 20 kV and distance of 6 cm. The pump feed rate was set to .01 µl/min using a 20 gauge needle.

Lastly, HA nanofibrous mats were produced using a 1:1 H_2O:DMF solvent system which also contained varying HA: phosphate salt weight ratios. Ratios were 1:1, 1:2 and 1:4. Salts included in the study were sodium phosphate, potassium phosphate, tripolyphosphate, and glycerol phosphate. HA was also electrospun using a similar 1:1 phosphate buffered saline (pH 7.4):DMF system. HA concentration was held constant at 1.5 w/v% for all trials while the electrospinning settings were as follows: Voltage was set to 15 kV and the collector plate distance was 6cm. The solution was fed through a 20 G needle at a rate of .005 µl/min.

3.3 CONDUCTIVITY

Solutions of various polymers were prepared at concentrations of 0.2, 0.4, 0.6, 0.8 and 1.0 w/v% both with and without the addition of a constant concentration of salts. Additionally, solutions were prepared in which the polymer concentration was held constant and the salt concentration varied. Conductivity measurements were made using an Oakton CON 510 conductivity meter (Figure 15). The meter was calibrated using 1413µS conductivity standard solution (potassium chloride, Fluka) prior to each use. Three successive measurements were taken at each concentration to obtain accurate data sets.

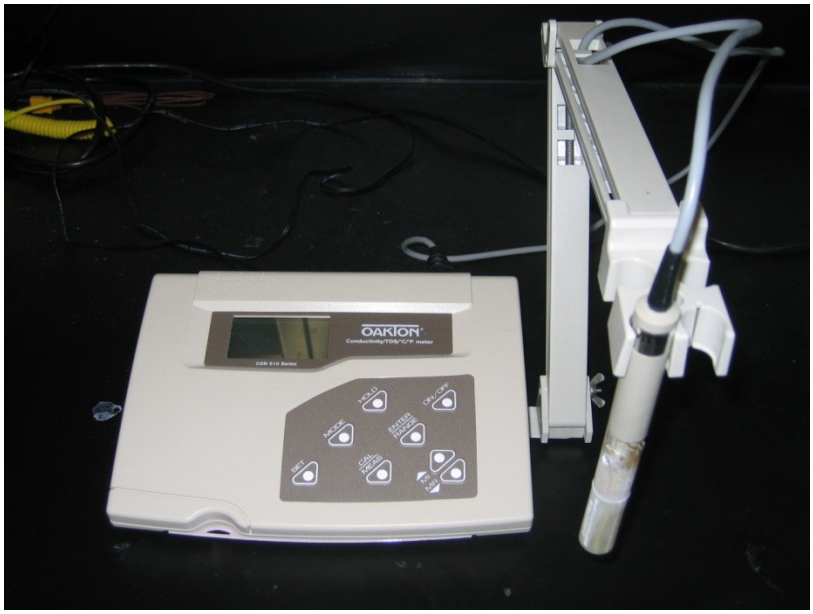

Figure 15: Oakton CON 510 Conductivity Meter

3.4 RHEOLOGY

In an attempt to correlate Rheology properties of various electrospinning solutions to electrospinnability, the viscosity of various polymer solutions were measured. Solutions of aqueous HA were prepared up to 4 w/v %. Solutions of medium molecular weight chitosan in 1% acetic acid and 1% TFA were also prepared in a similar fashion. Apparent viscosity measurements were taken using a TA Instruments AR2000 series rheometer. A concentric cylinder geometry of anodized aluminum with a stator inner radius of 15mm and a rotor of outer radius 14mm was used. Shear rate sweeps from 50 to 1100 per second were performed on all solutions, as well as their solvents, up to 4 w/v%. After 4 w/v%, a standard parallel plate geometry was used which including a 40 mm stainless steel plate. The experiment was repeated 3 times for each HA- phosphate salt solution as well as for HA in H_2O:DMF with no salt. Lastly, the procedure was also performed on solutions of HA in water and phosphate salts without DMF.

The apparent viscosity data was used to obtain specific viscosity according to the equation:

$$\eta_{sp} = \frac{\eta - \eta_0}{\eta_0} \quad (2)$$

where η is apparent viscosity of the solution and η_0 is the viscosity of the solvent. Specific viscosity was plotted versus shear rate to determine the regions of Newtonian behavior. Specific viscosity values at the same shear rate within this region were used for plotting specific viscosity versus concentration, where a change in slope denotes the change from the dilute unentangled to the semi-dilute entangled region.

3.5 SCANNING ELECTRON MICROSCOPY

Images of successfully electrospun nanofibrous mats were obtained using a Zeiss Supra 50/VP field emission scanning electron microscope (FESEM). The mats were sectioned and a Denton vacuum desk II sputtering machine was utilized to coat the samples for 10 s with platinum-palladium. SEM was also used to measure fiber diameters of the HA mats in basic solution. 50 random measurements were made throughout the section to obtain an accurate data set. ImageJ analysis software was utilized for fiber diameter measurements on SEM images of HA mats containing phosphate salts.

3.6 FOURIER TRANSFORM INFRARED SPECTROSCOPY

FTIR was used in various instances for the confirmation of chemical crosslinking as well as for the observation of chemical changes to the 3 w/v % HA in NaOH:DMF electrospinning solution. Spectra were obtained using an Excalibur FTS-3000 Fourier Transform spectrometer in transmission mode with resolution of 4 cm^{-1}. The software was set to perform 64 scans for each spectra within the range of 4000-500 cm^{-1}.

3.6.1 PELLET PREPARATION

As electrospinning of HA in a 4:1 0.5M NaOH:DMF solution became increasingly difficult when mixing time plus spinning time approached 30 minutes, FTIR was used to observe any chemical changes in HA that may have been taking place within that time window.

A large solution of 3 w/v % HA in 4:1 .5M NaOH was prepared (1.95g HA dissolved in mixture of 52 ml .5M NaOH and 13 ml DMF). At specific time intervals during mixing (5, 10, 20, 40, 60 and 80 minutes), aliquots of 10 ml were removed and immediately frozen via flash freezing in liquid nitrogen. The frozen solutions were then immediately lyophilized using a Flexi-Dry lyophilizer from FTS Systems (Stone Ridge, NY). The solutions were lyophilized for 24 hours at 48 mT and -84°C and a fine powder was obtained. The powder was used with potassium bromide (KBr) as background to form pellets for observation.

3.6.2 FILM AND FIBER PREPARATION

Crosslinking studies were performed on both electrospun fibrous mats and films of HA. Films were prepared by preparing a 1.5 w/v % aqueous solution of HA. The solution was spread onto glass microscope slides and allowed to dry at 25°C for 24 hours. The films were then peeled from the slides. Crosslinking was carried out with glutaraldehyde by utilizing a modified version of a two-step vapor crosslinking method previously developed by Schiffman *et al*. [25] As glutaraldehyde requires acidic conditions as a catalyst for crosslinking, one film was placed in a vapor chamber of acetic acid for 1 hour. For comparison, one film was not placed in acetic acid vapor. After acidic treatment, the films were immediately placed in a vapor chamber of glutaraldehyde overnight for at least 12 hours. Films were then removed and analyzed via FTIR to observe any evidence of chemical crosslinking.

Divinyl sulfone (DVS) was also used to crosslink HA fibrous mats by one step and two step methods. DVS requires alkaline conditions for crosslinking, and the electrospinning solution already contains NH_4OH, which should be sufficient to catalyze the crosslinking reaction. Just prior to electrospinning, DVS was added to the 1.5 w/v % HA in 2:1 NH_4OH:DMF spinning solution at HA:DVS weight ratios of 1:5 and 3:1. DVS was added to the solution and dispersed using a Vortex Genie (Scientific Industries, Inc., Bohemia, NY). Successfully produced mats were then removed from the collector plate, if possible, and analyzed via FTIR.

Alternatively, removable nanofibrous mats already produced using NaOH:DMF were used for crosslinking attempts via a two step method. The mats were placed in a

vapor chamber of DVS and allowed to crosslink for 24 hours. The mats were then removed and analyzed via FTIR to observe any chemical crosslinking.

3.7 ATR-FTIR

As the fibrous mats produced via phosphate salt addition as well as those using NH_4OH were extremely slow to accumulate, the mats could not be removed for traditional FTIR analysis. Therefore the collected fibers were scraped from the aluminum foil and analyzed using an ATR-FTIR. Spectra were obtained using a Smith's IlluminatIR ATR-FTIR with a resolution of $4cm^{-1}$. The ATR objective was composed of diamond with a numerical aperture of 0.71. The software was set to perform 64 scans within the range of 4000-500 cm^{-1}.

3.8 pH MEASUREMENT

pH was measured in NaOH, NH_4OH, and all salt-containing electrospinning solutions. Values were confirmed using pH paper with visual evidence recorded in the form of pictures.

CHAPTER 4: RESULTS AND DISCUSSION

4.1 PURE HA NANOFIBERS FROM BASIC SOLUTION

Fiber mats were reproduced using the NaOH:DMF solvent system outlined by Li *et al*. [50] While fibers could be produced using a 3 w/v % solution, there was a viscosity change observed in the solution over a certain time window. Solutions mixed overnight could not be electrospun the following day, although solutions mixed for less than 30 min were able to be electrospun. As the solution approached 30 min after mixing, there was an observed viscosity change which prevented electrospinning. SEM images of the electrospun mats at various time intervals are shown in Figure 16.

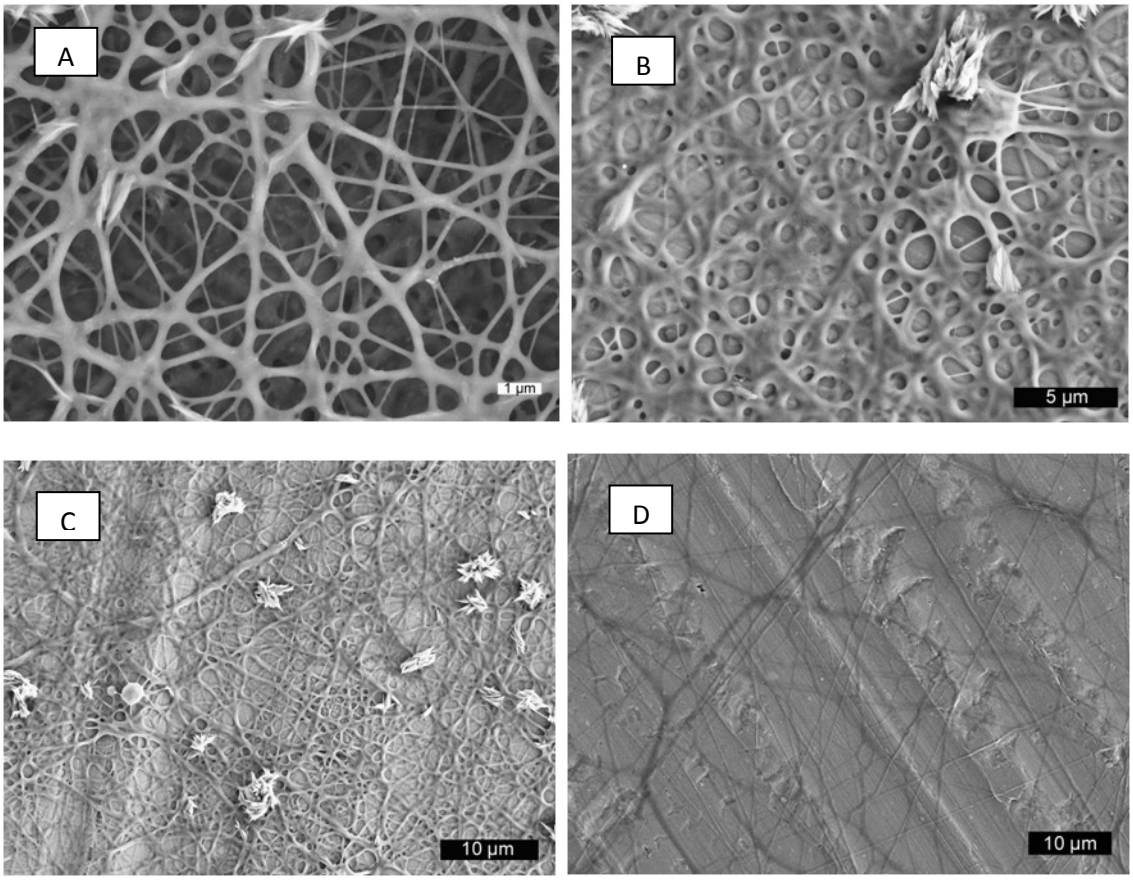

Figure 16: SEM Images of HA fibers from NaOH:DMF solutions at various mixing times: (A) 5 minutes, (B) 10 minutes, (C) 20 minutes, (D) 30 minutes

Continuous fiber mats are produced after 5 min mixing, with the quality of the mast decreasing as mixing time increases. At 30 min, the formation and collection of fibers is scarce. The average fiber diameter for HA solution mixed for 5 min was 224±81 nm, for 10 min was 477±210 nm, for 20 min was 377±127 nm, and for 30 min was 438±146 nm. Fiber distributions for these solutions are shown in Figure 17. There is no clear correlation between mixing time and fiber size, although the average fiber diameters among all the solutions is near 0.5 µm, and well beyond what is considered the "nanofiber" regime. By comparison, Li *et. al* reported fiber diameters of 198±45 nm

using a 10 wt% solution of HA. Although, they report no evidence of an electrospinning time window.

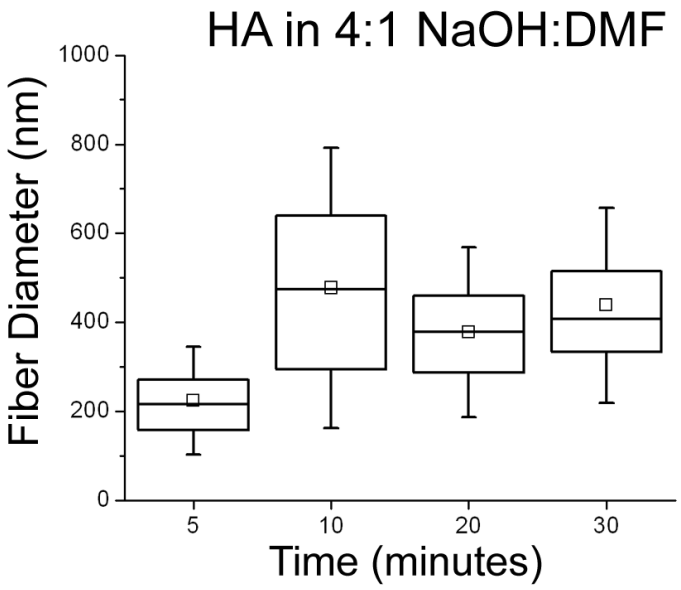

Figure 17: Fiber diameter distribution as a function of solution mixing time

The observed viscosity change of such strongly basic solutions may be correlated to the degradation of HA. The effect of pH on the viscosity behavior of HA in solution was recently studied by Maleki. [89] It was shown that HA solutions exhibited a decrease in viscosity when subject to extreme ends of the pH spectrum. Between pH 4 and 11, the solution viscosity remained relatively stable. Beyond these limits the decrease in viscosity was detected. They correlate this viscosity change to HA degradation, which has also been observed and confirmed by Tukita *et al.* [90] FTIR results of the solution at various time intervals, shown in Appendix D, are not definitive. The spectra obtained are inconclusive and they do not match any degradation mechanisms found in the literature.

Spectra with more definitive peaks must be obtained. Therefore more effective methods are necessary to observe and study this change.

In an effort to eliminate any degradation effects due to pH, the electrospinning of HA was attempted in a 2:1 NH_4OH:DMF solvent system. This solvent system was chosen to keep the possible positive effects of a basic solution on electrospinnability while using a weaker base. DMF was chosen again as it has been used to reduce the surface tension of many solutions in electrospinning. [50, 83] SEM images of 1.5 w/v % HA in this solvent system are shown in Figure 18.

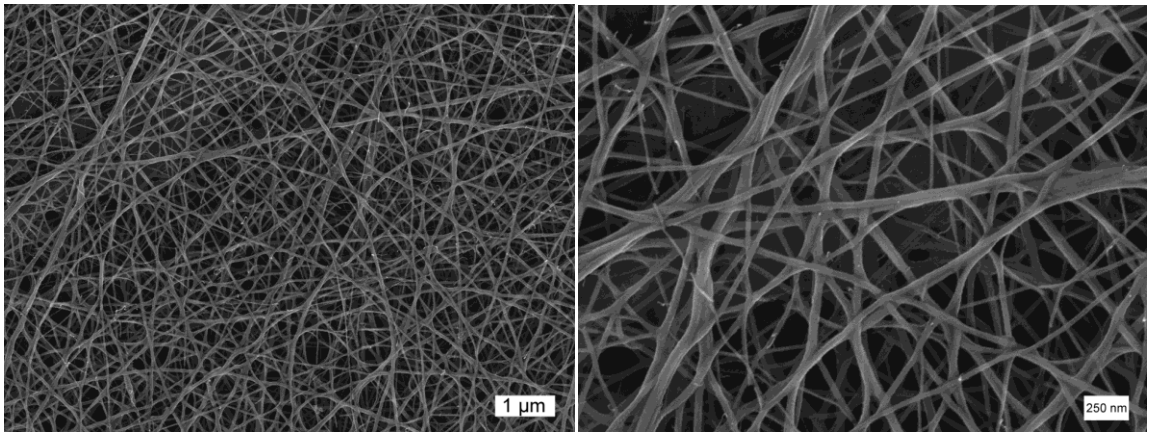

Figure 18: SEM images of 1.5 w/v % HA in 2:1 NH_4OH:DMF

Continuous, non-woven nanofibrous mats were produced as shown. Solutions showed no change in viscosity or electrospinning dependence on mixing time. The average fiber diameter of the mats was 39±12 nm, significantly lower than that of the mats produced by Li *et al.*[83] Fiber diameter distribution is shown in Figure 19 with comparison to fibers produced using NaOH:DMF (mixing time 5 minutes) as the solvent system. Fibers produced using NH_4OH:DMF exhibited an average diameter that is one order of magnitude smaller than those in NaOH:DMF.

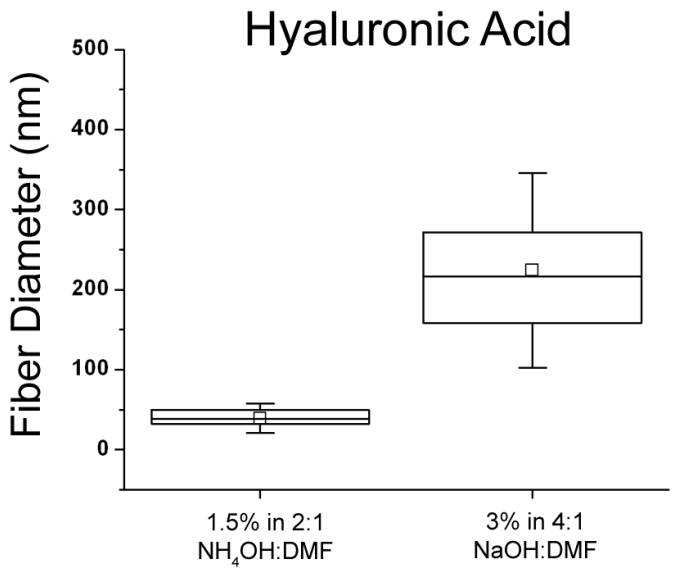

Figure 19: Fiber diameter distribution of pure HA nanofibrous mats in basic solutions

FTIR spectra of the nanofibrous mats obtained using NH_4OH:DMF are shown below in Figure 20. Characteristic peaks for HA are clearly evident and are listed in Table 3. Additionally, peaks for NH_3 as well as for DMF fail to present themselves clearly. Characteristic peaks for NH_3 are located near 1070 for stretching, 1650 for bending and 3200 for wagging. Similarly for DMF, characteristic peaks at 1675 for C=O and 3000-3300 for CH_3 are not clearly evident. The solvent to fiber ratio is too low in these samples for distinct peaks to show. This is encouraging as such solvents may pose a biocompatibility issue for several types of potential biomedical applications. Minimizing residual solvents like these is important.

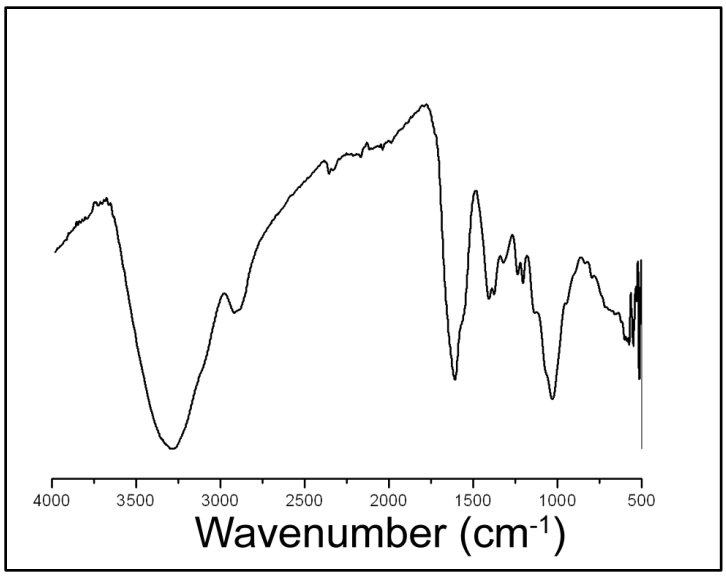

Figure 20: FTIR spectra of HA nanofibers in NH_4OH:DMF

Peak Range	Species
1375-1410	**C-O**
1560-1675	**C=O / C-N**
2800-2900	**C-H**
3200	**OH / N-H**

Table 3: Characteristic peaks for HA

4.2 PURE HA NANOFIBROUS MATS VIA PHOSPHATE SALT ADDITION

Despite the success of producing uniform fiber mats using NH_4OH:DMF, it remains a priority to utilize a solvent system which resembles an invert environment in terms of biocompatibility. While the NH_4OH:DMF exhibits a pH of around 11, this still remains fairly high and can limit the biomedically related applications in which such non-woven fibers can be used. Any undissolved solvent may still pose a biological threat should such fibers come into contact with a physiological system. In an effort to make a less toxic solvent system, the use of a H_2O:DMF mixed solvent was investigated. While this system has been reported to yield nanofibrous mats of pure HA in the literature, as mentioned earlier, these results could not be reproduced. The solution could not be electrospun. Therefore, the use of various phosphate salts was investigated to aid in electrospinning.

It is hypothesized that the phosphate salts will affect the electrospinning solution in a number of ways. Firstly, the salts will dissociate in an aqueous environment, causing a dramatic increase in the number of charge carriers in solution. These charge carriers may be available in the pendant drop for the creation of electrified jets. Secondly, they may help to balance the charge in the solution, allowing for a more uniform and homogenous distribution. Consequently, this may allow for the transformation of chains from a rigid rod-like orientation to one that is more flexible. As a result, entanglement will be increased, possibly shifting the entanglement concentration and allowing for more polymer to be incorporated at that concentration.

Additionally, evidence has shown that phosphates have the capability of crosslinking chitosan. Most work has focused on the ionic crosslinking capabilities with phosphates like tripolyphosphate (TPP). [91-93] But recently it has been shown that other phosphates can covalently crosslink via the hydroxyl groups in chitosan. Chenite *et al*. show that rapid gelation of chitosan is possible both at physiological conditions with glycerol phosphate. [94, 95] If this interaction can be applied to HA along with electrospinnability, it may provide for a one step-crosslinking method for producing crosslinked mats of pure HA.

4.2.1 HA NANOFIBERS VIA Na_2PO_4

SEM images of fiber mats produced from 1.5 w/v % HA in 1:1 H_2O:DMF with two different weight ratios of Na_2PO_4:HA are shown in Figure 21. Continuous, randomly oriented fibers are apparent in each case, although the abundance of branching is higher when less Na_2PO_4 is used. In addition, there appears to be the development of a film within the fiber matrix, causing a possible collapse of the fibers. The fiber surface morphology varies among the fiber mat. Fibers near the center of the image appear upraised with consistent circular structure. Conversely, fibers nearer the top of the image appear flattened and ribbon-like, with the surface of the fibers more uneven. With the higher Na_2PO_4:HA ratio the fibers are more rounded and independent, showing no significant range of morphologies.

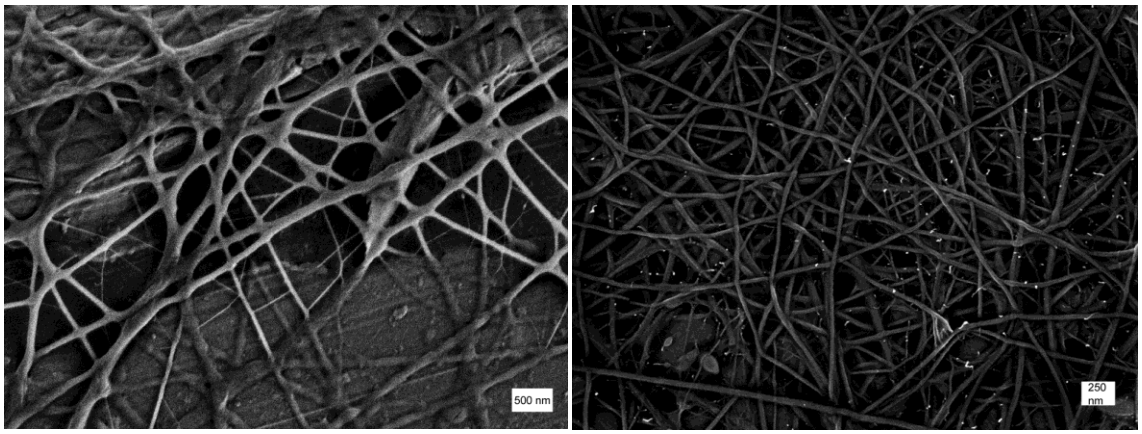

Figure 21: SEM Images of 1.5 w/v% HA in 1:1 H_2O:DMF with: 1:1 Na_2PO_4:HA (Left), 2:1 Na_2PO_4:HA (Right)

Fiber diameter distribution is shown in Figure 22. The average fiber diameter for the 1:1 Na_2PO_4:HA ratio was 104±38 nm. Similarly for the 2:1 ratio the average fiber diameter was 45±13 nm.

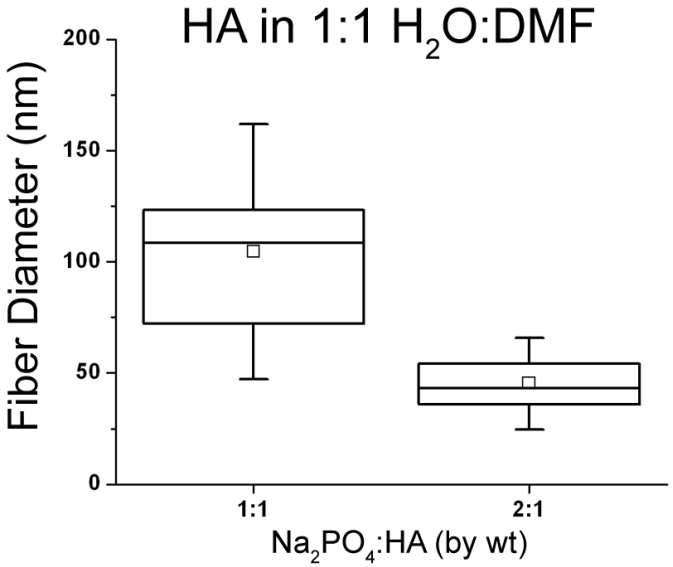

Figure 22: Fiber diameter distribution of HA nanofibrous mats using Na_2PO_4

4.2.2 HA NANOFIBERS VIA GLYCEROL PHOSPHATE

SEM images are given in Figure 23 of nanofibrous mats produced from solutions of 1:1 and 4:1 HA:GP by weight. It is interesting to note that cylindrical fiber formation is not apparent in the 1:1 sample. Rather, there is evidence of fibers collapsing and flattening onto the foil substrate. This significantly hinders the formation of a 3-D mat. The exact morphology of the fiber-like structures exhibited here has not been studied in the literature. Nanofibers that take the form of flattened ribbons, termed nanoribbons, have been reported. [96, 97] Additionally, the mechanism for the collapse of nanofibers has been outlined.[98] The morphologies demonstrated here fall between these descriptions. It was hypothesized that the ratio of HA:GP was too low and thus a 4:1 HA:GP ratio was attempted, which produced much more consistent fiber morphologies. The 4:1 sample shows a significant increase in the collection of fibers, along with significant branching. This correlates well with the sodium phosphate samples, as less salt also produced more branched fibers. Average fiber diameter for the 4:1 sample was 110±34 nm. Fiber diameters were not measured in the 1:1 sample as the structures formed cannot be accurately defined as fibers.

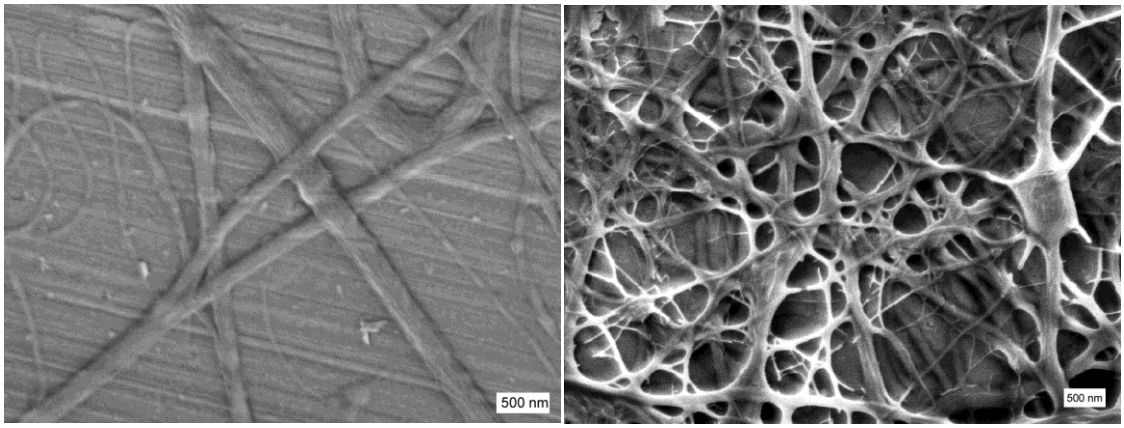

Figure 23: SEM images of HA nanofibers from 1:1 (left) and 4:1 (right) HA:GP solutions

4.2.3 HA NANOFIBERS VIA TRIPOLYPHOSHATE

SEM images of nanofibrous mats produced from solutions of 1:1 and 4:1 HA:TPP are given in Figure 24. Similar to the result obtained with GP, the 1:1 sample shows the same collapsed structure with a lack of significant accumulation. Again, a more uniform nanofibrous structure was obtained with a lower salt content. Although, the fibers produced from the 4:1 solution are more representative of cylindrical fibers. While there is evidence of some branching, it is not as prevalent as in other samples. The average fiber diameter of the 4:1 HA:TPP sample was 65±18 nm.

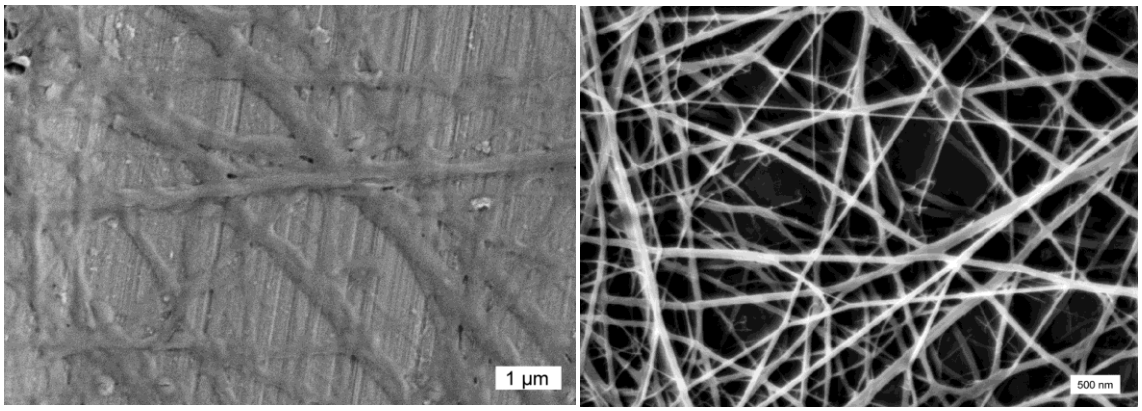

Figure 24: SEM images of HA nanofibers from 1:1 (left) and 4:1 (right) HA:TPP solutions

4.2.4 HA NANOFIBERS USING PBS:DMF SOLVENT SYSTEM

Common biological solutions such as PBS may provide the ability to expand the electrospinning of HA to include proteins and enzymes. With the previously described success of electrospinning HA utilizing phosphate containing solvents, a similar 1:1 PBS:DMF solvent was used. Initial studies have shown that the additional ions found in bought PBS solutions interfere with the electrospinning but more tests with lab created PBS will be done to elucidate the conditions. Fibers of HA could not be produced, but rather salt crystals were found on SEM samples prepared from these solutions. This is evident in Figure 25.

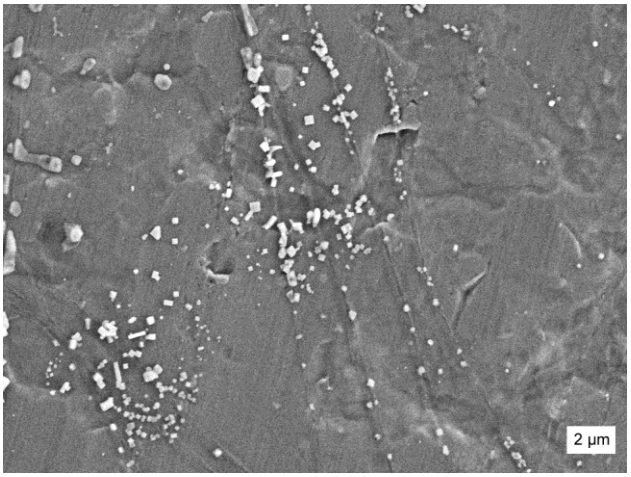

Figure 25: SEM image of salt crystals from electrospinning of HA in PBS:DMF

4.2.5 FIBER DIAMETER DISTRIBUTION FOR HA:PHOSPHATE SALT NANOFIBERS

Figure 26 shows the fiber diameter distribution for all HA nanofibrous mats produced with phosphate salts. Fibers produced using SP and TPP are nearly an order of magnitude smaller than those produced via NaOH:DMF. The best results, in terms of both average fiber diameter as well as overall consistency, are found in TPP and SP. Interestingly, better results were obtained with a higher salt concentration of SP and conversely with a smaller salt concentration in both GP and TPP. With such a small average fiber diameter with these solutions, as well as those in NH_4OH:DMF, collection of such fibers was extremely slow. In most cases, even after allowing for the electrospinning process to occur for several hours, collected fiber mats could not be removed from the foil collector. Easily observed, uniform coverage of the foil was observed however. Further investigation is required to optimize the system in order to

produce robust fiber mats. This may include more conductive collector materials and even dual syringe electrospinning to increase overall production.

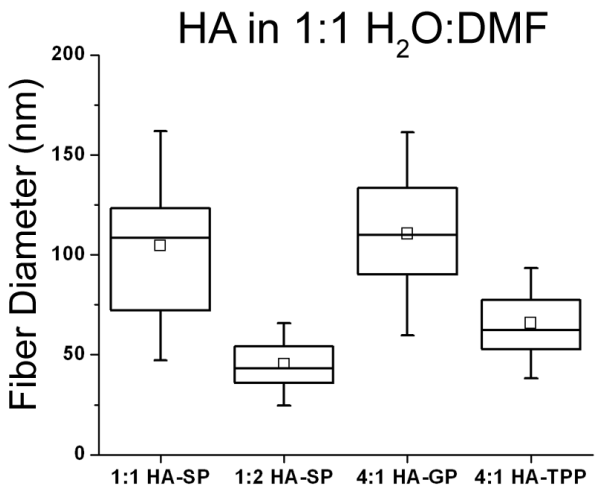

Figure 26: Fiber diameter distribution of HA fibers produced using phosphate salts

4.2.6 ATR-FTIR FOR HA:PHOSPHATE SALT NANOFIBERS

ATR-FTIR spectra for HA fibers produced with phosphate salts are shown in Figure 27. The characteristic peaks for HA, listed previously in Table 3, are clearly evident in these spectra as well.

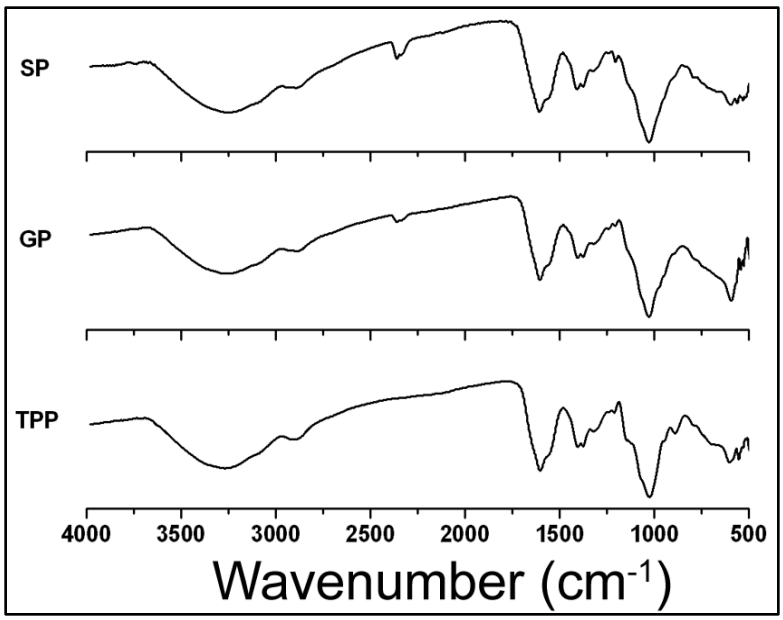

Figure 27: ATR-FTIR spectra for HA fibers with phosphate salts

In order to observe the binding of phosphates to HA, spectra of each salt were also obtained and compared to the HA fiber spectra. This allowed for possible detection of characteristic salt peaks in each of the HA fiber spectra. The spectra of the HA fibers and the salts were compared in the region between 900 and 400 cm^{-1} as this is the characteristic region for phosphorous-based peaks. The plots are shown in Appendix E.

The spectral comparisons do not show any evidence of phosphates bound to the HA fibers. The potential crosslinking of HA via these phosphates based on the observed gelation of chitosan was also sought here. The bonding mechanisms associated with this potential crosslinking was determined to be by the formation of a P-O-alkyl bond, designated by a broad peak at 1050-970 cm^{-1}. This peak is not evident in any of the spectra, confirming that crosslinking was unsuccessful. These results suggest that further studies are required to observe the exact interaction between the phosphate salts and the HA molecule.

4.3 pH OBSERVATIONS OF HA ELECTROSPINNING SOLUTIONS

The pH values observed for the solutions used are shown in Figure 28. The measurements shown were all performed on 1:1 HA:salt solutions, as the change to additional ratios did not show an observable change in pH. It is important to note the pH of the HA:TPP solution was between 7 and 8, giving the least toxic solution of all solutions tested, including those using NH_4OH. Additionally this value resembles that of physiological conditions, making it the leading potential candidate for biomedically related applications, such as wound healing dressings.

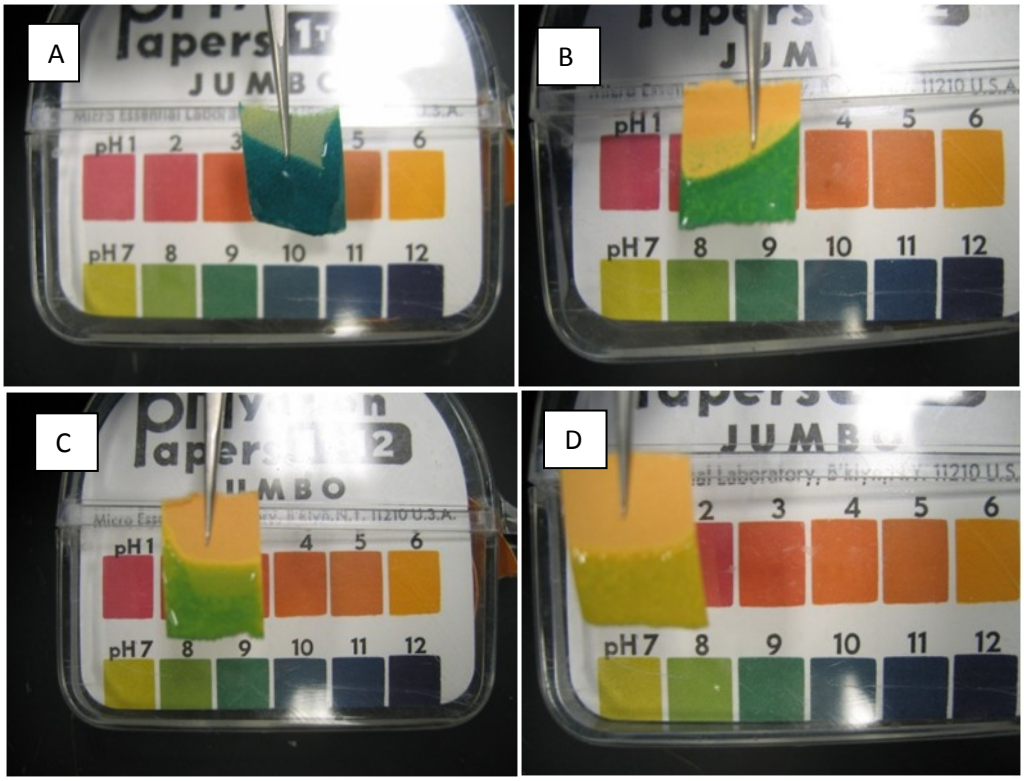

Figure 28: Observed pH values for various HA electrospinning solutions: 2:1 NH_4OH:DMF (A), 1:1 Na_2PO_4:HA (B), 1:1 GP:HA (C), 1:1 TPP:HA (D)

4.4 CONDUCTIVITY PROPERTIES OF ELECTROSPINNING SOLUTIONS

4.4.1 BASIC SOLUTIONS

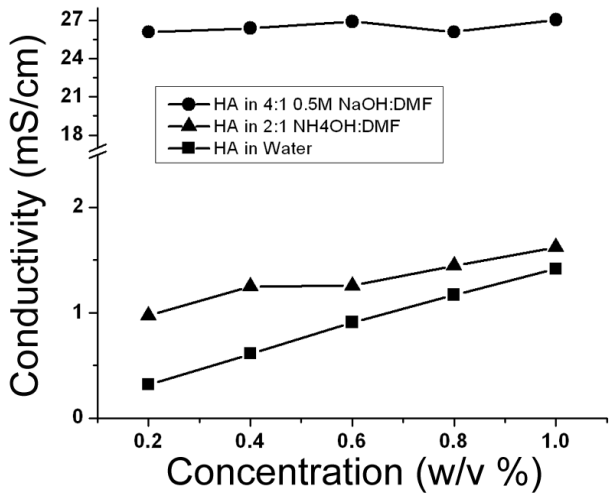

Figure 29: Conductivity of basic HA solutions

Conductivity values of both basic and aqueous solutions of HA are shown in Figure 29. Aqueous HA solution shows a distinct increasing linear trend, showing no signs of reaching a saturation point. Here, the effect of polymer concentration on conductivity is directly correlated. It is interesting to observe such a trend, as the HA used is a sodium salt. Similarly, for solutions of HA in ammonium hydroxide and DMF, the conductivity follows this linear trend. Although the conductivity is slightly higher, this can be attributed to the slight increase in concentration of charge carriers in solution. Lastly, noting the break in the graph, the solutions of HA in sodium hydroxide and DMF show the highest conductivity. This extreme increase in conductivity can be attributed to the higher dissociation of NaOH into its respective ions of Na^+ and OH^- in solution. It is also interesting to note that the effect of polymer concentration on the conductivity is

minimal, with the values remaining fairly constant. This extreme difference in conductivity, combined with the fact that both basic solutions allowed for successful electrospinning, shows that highly conductive solutions are not solely required for successful electrospinning.

4.4.2 PHOSPHATE SALT SOLUTIONS

Conductivities for HA in solutions containing phosphate salts are shown in Figure 30. Aqueous HA data is reproduced here. The sodium phosphate containing solution is the only solution demonstrating a higher conductivity than HA in water, along with an increasing trend. The TPP containing solution also shows in increasing linear trend, although the conductivity is lower than that of aqueous HA. Lastly, for the sodium phosphate containing solution, the conductivity appears to have reached a constant value, with a limited effect of polymer concentration. Again, considering that each of these solutions were successfully electrospun, this shows that high solution conductivity is not exclusively required for electrospinning. These results may indicate a potential interaction between the free phosphate ions in solution with the HA chains. It was expected that a higher solution conductivity would be observed in all solutions. While this is the case for GP containing solutions, the remaining solutions did not show significant increases. Thus, the free phosphate ions may be saturating the HA chains, removing them as free charge carriers.

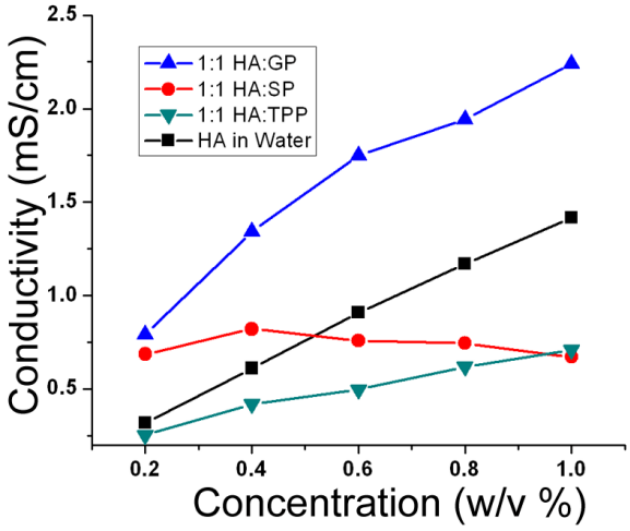

Figure 30: Conductivity of phosphate salt-containing HA solutions

4.4.3 ADDITIONAL SALT SOLUTIONS

HA solutions were prepared using additional sodium salts of different anion sizes and ionic strengths. In this case, the polymer concentration was held constant at 0.5 w/v% and the salt concentration varied. Figure 31 shows the results of the conductivity measurements. Both sodium phosphate and sodium sulfate show a minimal effect of salt concentration on conductivity. In contrast, solutions containing higher concentrations of sodium chloride consequently display a higher conductivity.

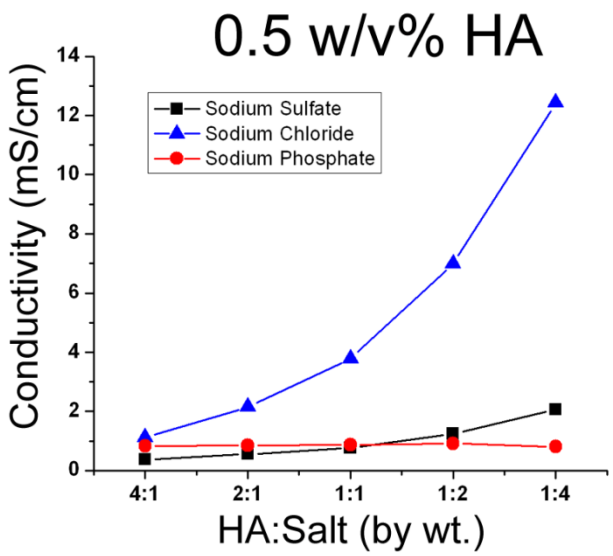

Figure 31: Conductivity of HA solutions with various sodium salts

The ionic strength is higher in the sulfate and phosphate salts than with the chloride salt and in addition the chloride salt has a much smaller radius. The results not only suggest a potential ionic strength effect on conductivity, but also an anion size dependence. The radius of the chloride ion is 1.81 Å while the apparent ionic radii for sulfate and phosphate ions are 2.3 Å and 2.38 Å, respectively.[99] The results suggest that a smaller ionic radius and a lower ionic strength may allow for the observed increases in conductivity with sodium chloride. A potential reason for this increase can be developed. Under normal aqueous conditions in the semi-dilute region, there is a strong hydrogen bonding effect between water molecules and the HA molecule. This effectively creates a water cloud surrounding the sodium HA chains, including the carboxyl groups which are saturated by sodium ions. The chloride ions seem to be having a larger effect on the bound water than that of the larger phosphate or sulfate ions. This ultimately leads

to the observed increase in conductivity. Although the exact effects of the salts are not fully understood at this time.

4.5 RHEOLOGICAL OBSERVATIONS

Viscosity measurements were made on aqueous HA and H_2O:DMF solutions containing phosphate salts in order to determine any changes to entanglement resulting from the solvents or salt addition. As mentioned earlier, it was hypothesized that stronger solvents, including those with added salts, will allow for the transition of the polymer chains from rigid rods to a more entangled or more incorporated form. This may be evident in a shift of the entanglement concentration. Additionally, the charges in solution may interact with the chains and potentially neutralize any electrostatic interactions causing the observed high viscosity in aqueous environments.

4.5.1 AQUEOUS HA

The apparent viscosity as a function of shear rate for aqueous HA is shown in Figure 32. The results show a traditional shear thinning response. Similar plots for HA in H_2O:DMF and with phosphate salts, available in Appendix F, also show the same property.

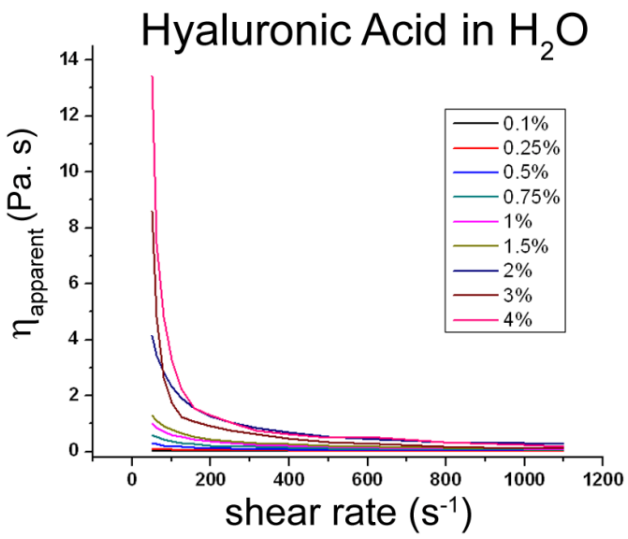

Figure 32: Apparent viscosity versus shear rate for aqueous HA

The recorded apparent viscosity data for each solution was transformed to specific viscosity according to Equation 2. The results were plotted versus shear rate on a log-log scale, shown in Figure 33. Similar plots for HA in H_2O:DMF and with phosphate salts are available in Appendix G. There is a clear transition visible between the Newtonian region and the shear thinning region. In most cases, the experiment was not run to high enough shear rates to observe the transition back to Newtonian behavior. As mentioned earlier, all viscosity values were taken from the Newtonian region, specifically at a shear rate of 62.95 s^{-1}. It can be seen that the transition between the regions begins to breakdown with the higher concentration solutions, especially at high shear rates. Such deviation can be a result of spin out. Viscosity values chosen in the Newtonian region were not affected by this deviation.

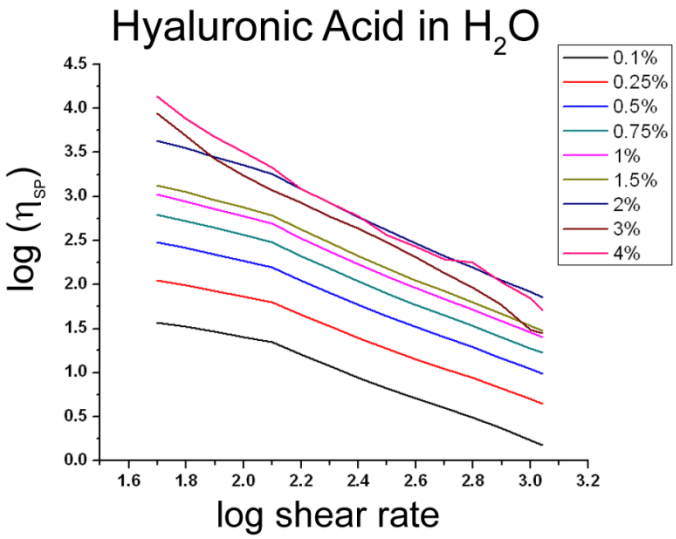

Figure 33: Specific viscosity versus shear rate for aqueous HA

Specific viscosity versus concentration for aqueous HA is shown in Figure 34. According to theory, the transition from the semi-dilute unentangled region to the semi-dilute entangled region is denoted by the change in slope. It was expected that the entanglement concentration would present near 0.5% as 2-2.5 times this value would give the concentration used in this work to produce bead-free fibrous mats of HA. McKee *et al.* found that in order to produce bead free nanofibers from polymer solutions, the polymer concentration should be 2-2.5 times the entanglement concentration.[100] For this reason entanglement was sought in this region. Although, according to theory on neutral polymers, the unentangled region should follow a slope of 1 while the entangled region should follow with a slope of 4. If the entanglement concentration is set at 0.5%, as shown in Figure 34, the slopes do not follow the expected theoretical values. The plot obtained here does not follow the expected theoretical results.

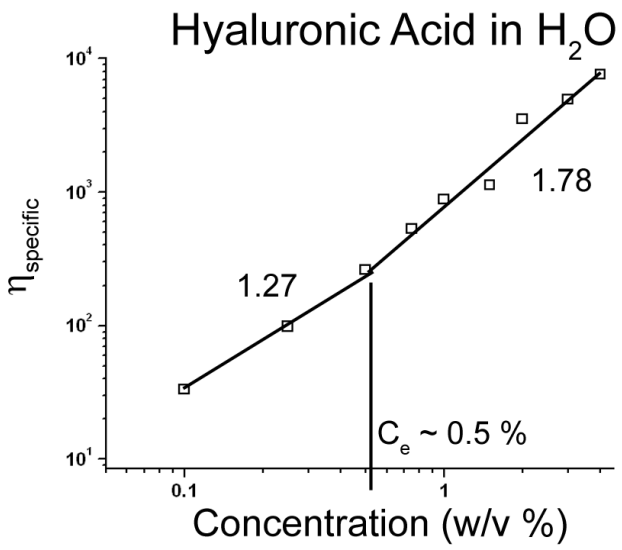

Figure 34: Entanglement concentration for aqueous HA

It was thought that stronger solvents may play an important role in affecting the concentration at which entanglement takes place. This was based on previous work by Klossner *et al.* on chitosan solutions. They showed a chitosan entanglement concentration of 3 wt. % in a solvent containing 80% acetic acid. [101] In our lab, Schiffman *et al.* performed rheological measurements on chitosan solutions in 1% acetic acid solutions. It was hypothesized that a lower concentration of acetic acid would lower the entanglement concentration below the 3% observed by Klossner *et al*. Although, the results were also inconclusive, similar to the aqueous HA plot, with no entanglement concentration clearly observed. [102]

4.5.2 HA IN WATER WITH PHOSPHATE SALTS

Phosphate salts were added to the aqueous HA solutions to determine any effects on entanglement. The previous results show that aqueous solutions of HA do not follow the solution entanglement theory. The results obtained are similar, with no change in

slope strong enough to classify a specific entanglement concentration. The plots are shown in Figure 35. The sodium phosphate plot shown was also expanded to include concentrations higher than 4 w/v% and lower than 0.75% to determine if the entanglement concentration was located outside the bounds of the original concentration range. The results obtained were similar, showing no distinct entanglement concentration.

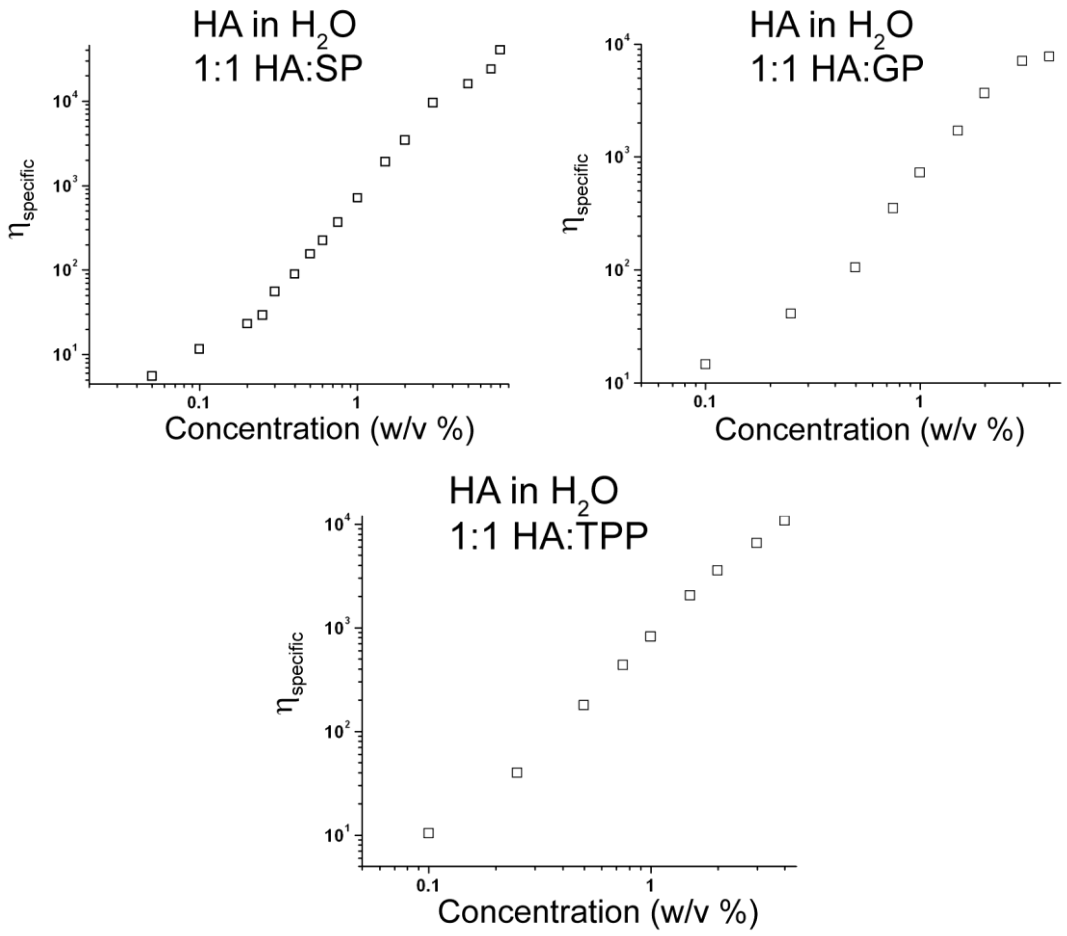

Figure 35: Entanglement concentrations for solutions of HA in water with added phosphate salts

4.5.3 HA IN WATER:DMF WITH PHOSPHATE SALTS

An attempt to observe a change in entanglement concentration was carried out with HA-phosphate salt solutions in H_2O:DMF. The specific viscosity versus concentration plot (0.05 to 8 w/v%) for HA in H_2O:DMF is shown in Figure 36. Again, there is no observed change in slope that is strong enough to denote a transition between entanglement regions. Similar to the aqueous HA plot, the correlation is linear between viscosity and concentration, even when the concentration region was expanded up to 8 w/v%.

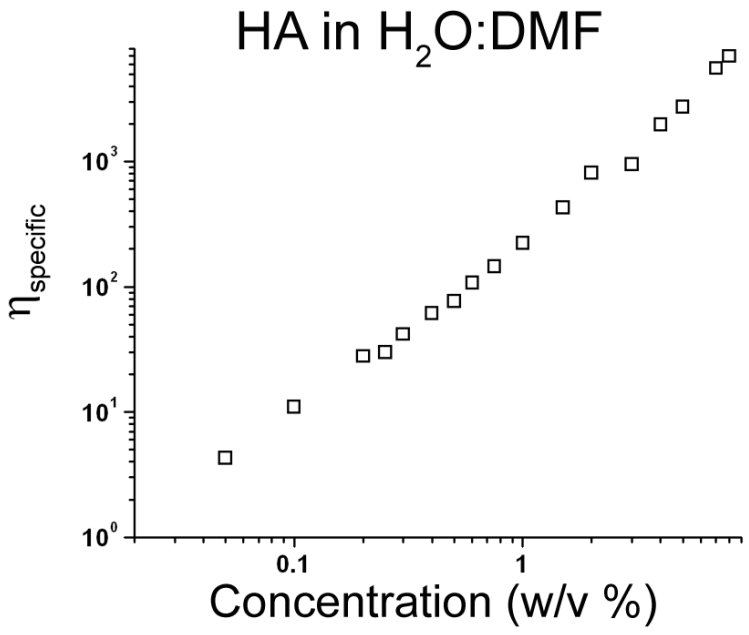

Figure 36: Specific viscosity versus concentration for HA in 1:1 water:DMF

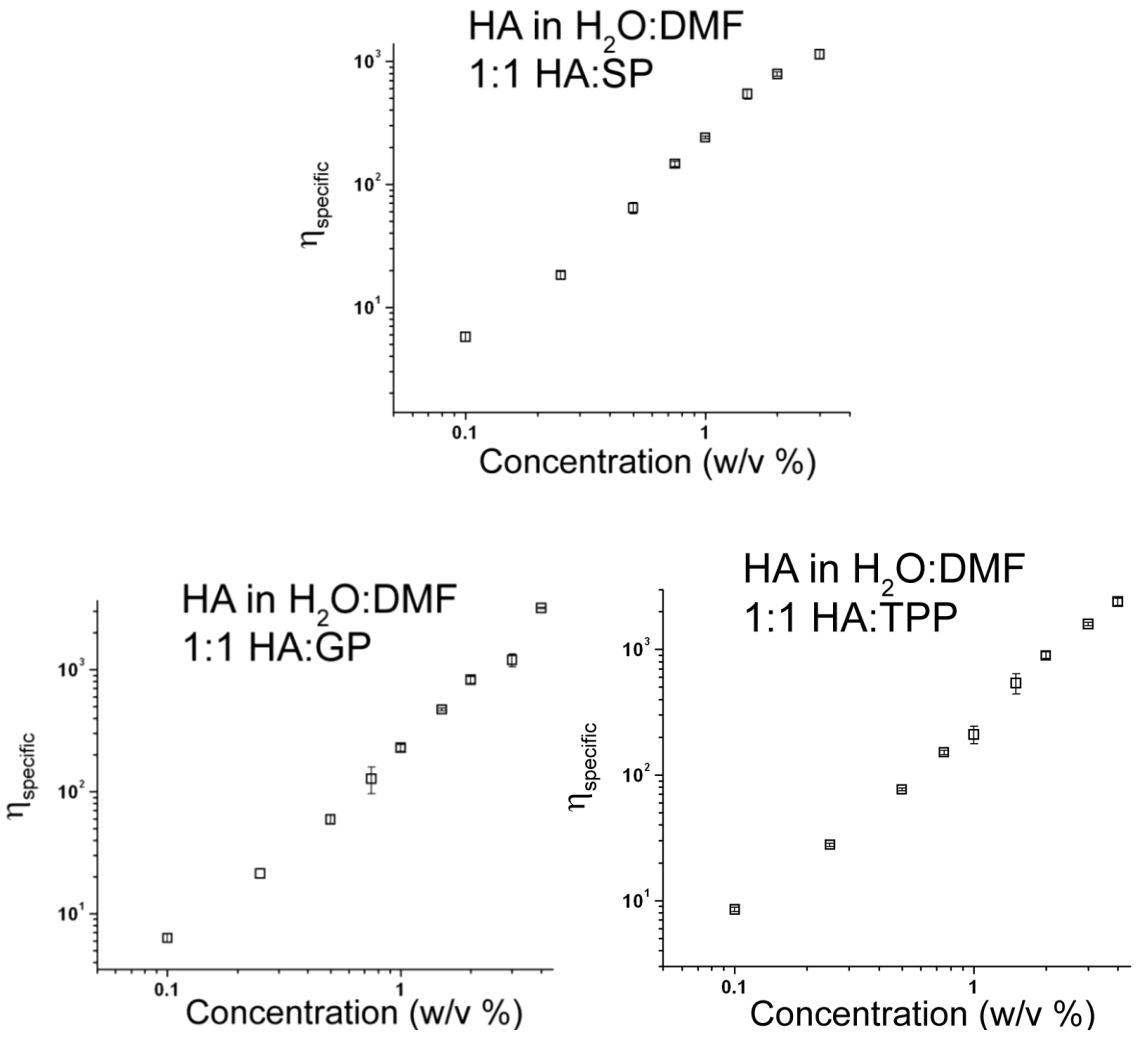

Figure 37: Specific viscosity versus concentration for HA in 1:1 water:DMF with phosphates

Figure 37 shows similar plots for HA in H_2O:DMF with the addition of phosphate salts. A linear relationship is observed in all solutions, with no entanglement concentration visible within the concentration range. The SP plot was then expanded to include concentrations both higher than 4 w/v% and lower than 0.75%, similar to that of HA in H_2O:DMF shown in Figure 36. It was hypothesized that the entanglement concentration may have been outside the bounds of the original plot. The expanded plot

is shown in Figure 38. A stronger change in slope, closer in resemblance to theory, is observed around 3 w/v%. The entanglement concentration becomes evident here in a solvent system constructed from 3 different components: water, DMF and sodium phosphate.

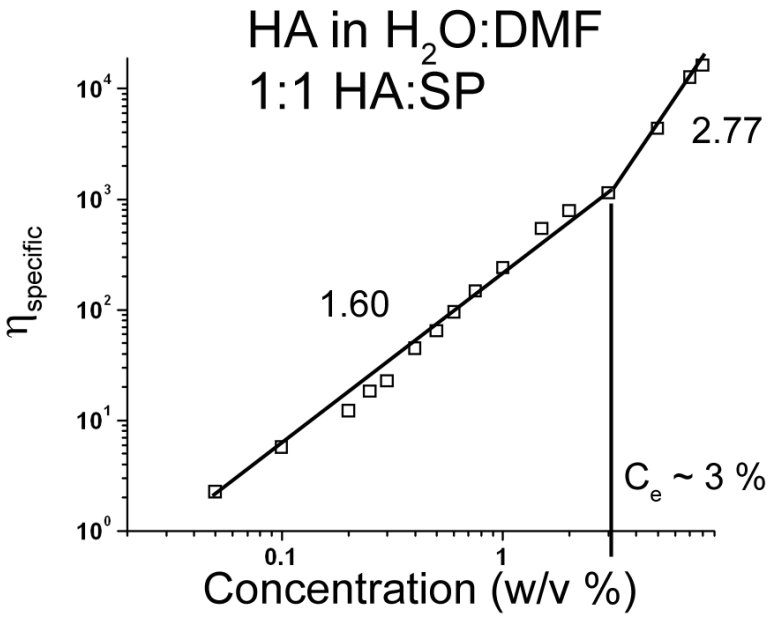

Figure 38: Specific viscosity versus concentration for HA in 1:1 water:DMF with sodium phosphate

The appearance of an entanglement concentration correlates well with our electrospinning solutions. Electrospinning was only possible in our electrospinning setup when an HA solution was constructed using three components. We could not reproduce literature nanofibers produced using only two components by Li *et al.* from H_2O:DMF.[83] Additionally, the electrospinning of simple aqueous HA solutions has yet to be shown in the literature. Electrospinning was only possible in the solvent system utilizing H_2O, DMF as well as phosphate salts, like sodium phosphate, or sodium

hydroxide and ammonium hydroxide. Again, this correlates well with the appearance of an entanglement concentration shown in Figure 37. Entanglement was only achieved when all three components are present. These results, though, do not predict if one component is more effective than another in achieving entanglement. Additionally, determining the exact role that each component plays in allowing for entanglement as well as successful electrospinning is difficult. This is because the system utilizes all three components simultaneously.

CHAPTER 5: CONCLUSION

Nanofibrous mats of HA were successfully produced in a standard electrospinning setup and without the use of a blended polymer to increase electrospinnability. Table 4 summarizes the solutions used and fiber diameters for the resulting fiber mats. Included are the results of electrospinning of HA from the literature for comparison. Successful mats were produced in basic solution using NaOH (pH 13) as well as NH_4OH (pH 10). Fibers reproduced using NaOH were similar in diameter to those in the literature. Although, it was shown that mixing time greatly affected the spinnability of HA in NaOH due to the possible degradation of HA in such strongly basic solution. Fibrous mats produced in less basic NH_4OH showed no signs of time dependence, with a much smaller average fiber diameter at less than 100 nm. Additionally, the residual solvents, NH_4OH and DMF were in such small ratios compared to the fibers produced that their characteristic peaks were not distinctly observed in the IR spectra of the fibers. This is extremely important for potential biomedical applications that would require non-toxic materials.

Polymer Concentration	Solvent	Salt	Average Fiber Diameter	Reference
3 w/v % HA	4:1 0.5M NaOH:DMF	N/A	224±81 nm	N/A
1.5 w/v % HA	2:1 NH_4OH:DMF	N/A	39±12 nm	N/A
1.5 w/v % HA	1:1 H_2O:DMF	2:1 SP:HA	104±38 nm	N/A
1.5 w/v % HA	1:1 H_2O:DMF	1:4 GP:HA	110±34 nm	N/A
1.5 w/v % HA	1:1 H_2O:DMF	1:4 TPP:HA	65±18 nm	N/A
1.5 w/v % HA	1:1 H_2O:DMF	N/A	200 nm	[83]
10 wt% HA	4:1 0.5M NaOH:DMF	N/A	198±45	[50]

Table 4: Summary of successfully produced fiber mats

While production of pure HA nanofibrous mats was possible in basic solutions, it was also concluded that the addition of phosphate salts to an H_2O:DMF solution also enhanced the electrospinnability of HA. Nanofibrous mats were produced in near neutral solutions using three different phosphate salts: sodium phosphate, glycerol phosphate, and tripolyphosphate. While a 2:1 salt:HA ratio was required for solutions containing SP to electrospin, it was found that GP and TPP solutions required a much lower ratio at 1:4. This may be due to the increased complexity of the TPP and GP salts. In each case, fibers were produced with an average near or below 100 nm, again significantly improving upon the limited previous literature. While successful mats were produced, the collection of the fibers was extremely slow, producing mats that were not able to be removed from the foil even after extended spinning times. Additionally, IR spectra did not show the interaction between the HA molecule and the phosphate salts. More work is needed to

optimize the system to increase collection as well as to observe the exact effect the phosphate salts have on the HA chains.

Results show that the conductivity of HA in aqueous solution follows an increasing linear trend with concentration while in NaOH:DMF the conductivity is constant with increasing concentration. Additionally, the conductivity is significantly higher. Conversely with NH_4OH the conductivity is only slightly higher than that of aqueous HA and follows the same trend. The addition of phosphate salts has several different effects on the conductivity. HA with GP shows a slight increase in conductivity while solutions containing TPP show a slight decrease in conductivity. Solutions with SP showed limited variation with concentration, with conductivity remaining fairly constant. It was expected that the conductivity would increase more significantly with the addition of salts, although the results suggest more of an interaction of the salts with the HA chains, removing them from the solution. More importantly, the results, along with successful electrospinning, show that solutions with increased conductivity are not solely required for the electrospinning of natural polyelectrolytes.

Rheological observations suggest that a solvent system that is composed of three components, H_2O, DMF and either phosphate salts, NH_4OH, or NaOH is required for the observation of entanglement at low concentrations, and additionally for successful electrospinning. Entanglement concentrations were not visible in solutions composed of simply one or two of these components, such as water, water and DMF, or water and phosphate salts. But solutions of HA in H_2O:DMF with sodium phosphate do show a change from the unentangled to the entangled region that more closely resembles that of theory.

CHAPTER 6: FUTURE WORK

6.1 OPTIMIZATION AND ELECTROSPINNING OF ALGINATE

In order to produce useful nanofibrous mats, the electrospinning solvent systems and settings must be optimized. As mentioned previously, all mats produced using NH_4OH and phosphate salts involved the extremely slow collection of fibers. Robust fiber mats which can be removed from the collecting material are essential for any commercial applications. Therefore, optimization is a key requirement. In this process, the minimum amount of phosphate salt required for successful electrospinning may be investigated as well as DMF in solution. Limiting these additional variables not only decreases cost, but can also increase biocompatibility in the case of DMF.

The exact interaction and effect that DMF has on the HA molecule in solution must be confirmed. This will further the understanding of electrospinning of natural polymers. Additionally, the same holds for the phosphate salts. Better protocols must be developed in order to observe the interactions.

In addition, due to the similarities of the molecules of HA and alginate, many of the successful methods found in this work can be applied to alginate in hopes of producing pure nanofibrous mats. As mentioned previously, like HA, alginate has proven equally as difficult to electrospin without the aid of synthetic polymers in a blend. Members of the NPP lab are currently investigating this problem.

6.2 CROSSLINKING OF HA

Equally important to producing thicker, robust HA nanofibrous mats, is the successful chemical crosslinking of HA in bulk as well as in fiber form. If nanofibrous mats are to be used in aqueous environments or are to come into contact with biological fluids such as blood plasma, it is important that they retain their structure and do not dissolve. Chemical crosslinking will prevent this. This research involved preliminary work investigating the crosslinking of HA using two common crosslinkers, glutaraldehyde and divinyl sulfone (DVS).

6.2.1 DIVINYL SULFONE

As mentioned earlier, it has been shown in the literature that divinyl sulfone can chemically crosslink HA.[46] DVS has been chosen as an ideal crosslinking agent for several reasons. Firstly, without any deacetylation, HA does not contain any free amine groups that are typically required for many crosslinking reactions. DVS crosslinks via the primary hydroxyl groups, forming sulfonyl bisethyl bonds. Secondly, the DVS crosslinking reaction requires alkaline conditions to proceed. Two of the solvent systems we have shown to be successful in producing nanofibrous mats are basic. This provides for the possibility of an ideal one-step crosslinking mechanism, where HA is crosslinked during the electrospinning process.

The FTIR results obtained for one step (3:1 and 1:5) and two step (overnight) crosslinking of nanofibrous mats produced using NH_4OH:DMF are shown in Figure 39. The spectra lack the definition to deduce any crosslinking effects. Although, simple

solubility tests of the mats in deionized water showed no signs of crosslinking, as the mats dissolved when submerged. It is interesting to note that collection of the HA nanofibers using crosslinker was enhanced, as the fibers were removed from the foil. While this proved positive, successful crosslinking was not definitive. A more detailed investigation into the proper HA:DVS ratio, as well as the effect, if any, of the crosslinker on the conductivity of electrospinning solution will be investigated in future work.

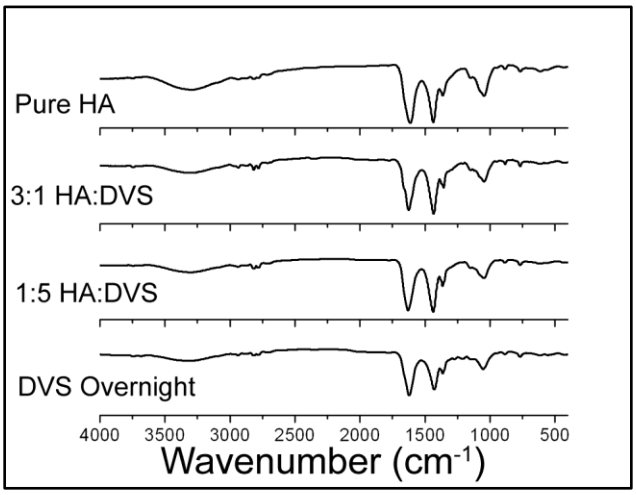

Figure 39: FTIR results of HA fiber mats crosslinked with DVS

Lastly, SEM images of the nanofibrous mats produced with DVS are shown in Figure 40. The images show the emergence of a film, possibly excess DVS, on the surface of the mats. This is most clearly evident with the higher amount of DVS. Although, the addition of DVS to the solution did not appear to have an effect on the overall electrospinnability of either solution.

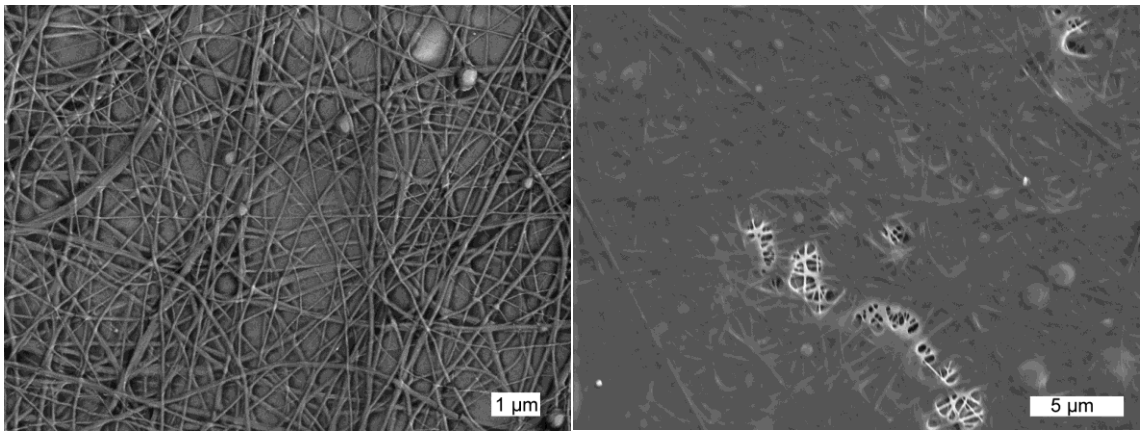

Figure 40: SEM images of HA fiber mats produced with: 3:1 HA:DVS (left) and 1:5 HA:DVS(right)

Fiber diameter distribution is shown in Figure 41 as well. With increasing amount of DVS in solution, the overall fiber diameter increases dramatically. There may exist a tradeoff between average fiber diameter and the ability to crosslink. This correlation will be investigated in future work as well.

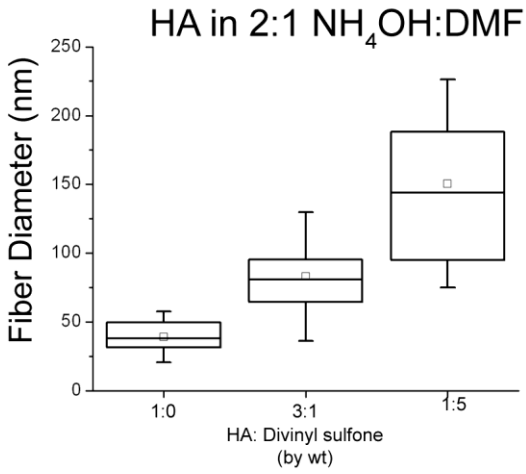

Figure 41: Fiber diameter distribution for HA nanofibrous mats with DVS

6.2.2 GLUTARALDEHYDE

FTIR results utilizing glutaraldehyde are shown in Figure 42. HA films were subjected to acetic acid (AA) for one hour prior to glutaraldehyde (GA) vapor treatment in order to catalyze the crosslinking reaction. The IR results do not show conclusive evidence of crosslinking and thus better spectra are needed to observe the chemical change. While basic solubility tests in water did not show permanent crosslinking, the films crosslinked with AA pre-treatment did remain undissolved for 2-3 minutes versus immediate dissolution without any AA. These results look promising and a more detailed study, including extended AA pre-treatment times, will be included in future work.

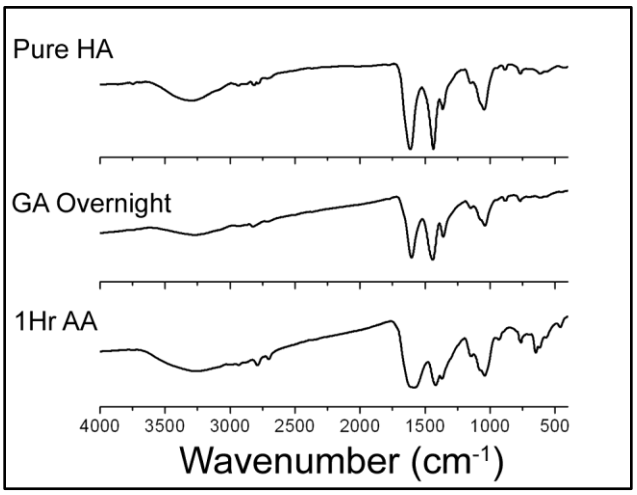

Figure 42: FTIR results of HA fiber mats crosslinked with GA

CHAPTER 7: REFERENCES

1. Vaseashta, A., *Green Nanotechnologies For Responsible Manufacturing.*

2. Bogaert, J. and P. Coszach. *Poly (lactic acids): a potential solution to plastic waste dilemma*. 2000: Wiley-VCH; 1999.

3. Demirbas, A., *Pyrolysis of municipal plastic wastes for recovery of gasoline-range hydrocarbons.* Journal of Analytical and Applied Pyrolysis, 2004. **72**(1): p. 97-102.

4. Pinto, F., et al., *Pyrolysis of plastic wastes. 1. Effect of plastic waste composition on product yield.* Journal of Analytical and Applied Pyrolysis, 1999. **51**(1-2): p. 39-55.

5. Tombs, M. and S. Harding, *An Introduction to Polysaccharide Biotechnology*. 1998: CRC Press.

6. Brant, D., *Solution properties of polysaccharides*: American Chemical Society.

7. Rees, D., *Polysaccharide Shapes*. 1977: Chapman & Hall.

8. Kumar, M., *Chitin and chitosan fibres: a review.* Bull. Mater. Sci, 1999. **22**: p. 905–911.

9. Min, B.-M., et al., *Chitin and chitosan nanofibers: electrospinning of chitin and deacetylation of chitin nanofibers.* Polymer, 2004. **45**(21): p. 7137-7142.

10. Cutler, H., A.C.S.D.o. Agrochemicals, and A.C.S. Meeting, *Biologically Active Natural Products: Potential Use in Agriculture*. 1988: American Chemical Society.

11. Ravi Kumar, M., *A review of chitin and chitosan applications.* Reactive and Functional Polymers, 2000. **46**(1): p. 1-27.

12. Austin, P. and C. Brine, *Chitin films and fibers*. 1977, US Patent 4,029,727.

13. Francis Suh, J. and H. Matthew, *Application of chitosan-based polysaccharide biomaterials in cartilage tissue engineering: a review.* Biomaterials, 2000. **21**(24): p. 2589-2598.

14. Agboh, O. and Y. Qin, *Chitin and Chitosan Fibers.* Polymers for Advanced Technologies, 1997. **8**: p. 355-365.

15. Laudenslager, M., *Chitosan and carboxymethyl chitosan as catalyst matrix materials*. 2008, Drexel University.

16. McKee, M., et al., *Solution rheological behavior and electrospinning of cationic polyelectrolytes.* Macromolecules, 2006. **39**(2): p. 575-583.

17. Schiffman, J. and C. Schauer, *Cross-linking chitosan nanofibers.* Biomacromolecules, 2007. **8**(2): p. 594-601.

18. Welsh, E., et al., *Chitosan Cross-Linking with a Water-Soluble, Blocked Diisocyanate. 1. Solid State.* BIOMACROMOLECULES-WASHINGTON-, 2002. **3**(6): p. 1370-1374.

19. WEI, Y., et al., *The crosslinking of chitosan fibers.* Journal of polymer science. Part A. Polymer chemistry, 1992. **30**(10): p. 2187-2193.

20. Berger, J., et al., *Structure and interactions in covalently and ionically crosslinked chitosan hydrogels for biomedical applications.* European Journal of Pharmaceutics and Biopharmaceutics, 2004. **57**(1): p. 19-34.

21. da Silva, R., et al., *Transport of Small Anionic and Neutral Solutes through Chitosan Membranes: Dependence on Cross-Linking and Chelation of Divalent Cations.* Biomacromolecules, 2008.

22. Desai, K., et al., *Morphological and Surface Properties of Electrospun Chitosan Nanofibers.* Biomacromolecules, 2008. **9**(3): p. 1000-1006.

23. Chen, J.-P., G.-Y. Chang, and J.-K. Chen, *Electrospun collagen/chitosan nanofibrous membrane as wound dressing.* Colloids and Surfaces A: Physicochemical and Engineering Aspects, 2008. **313-314**: p. 183-188.

24. Du, J. and Y.-L. Hsieh, *Nanofibrous membranes from aqueous electrospinning of carboxymethyl chitosan.* Nanotechnology, 2008. **19**(12): p. 125707/1-125707/9.

25. Schiffman, J. and C. Schauer, *One-Step Electrospinning of Cross-Linked Chitosan Fibers.* Biomacromolecules, 2007. **8**(9): p. 2665-2667.

26. Matsuda, A., et al., *Preparation of Chitosan Nanofiber Tube by Electrospinning.* Journal of Nanoscience and Nanotechnology, 2007. **7**(3): p. 852-855.

27. Greiner, A. and J. Wendorff, *Electrospinning: a fascinating method for the preparation of ultrathin fibers.* Angew Chem Int Ed, 2007. **46**: p. 5670–5703.

28. Pham, Q., U. Sharma, and A. Mikos, *Electrospinning of Polymeric Nanofibers for Tissue Engineering Applications: A Review.* Tissue Engineering, 2006. **12**(5): p. 1197-1211.

29. Duan, B., et al., *Degradation of electrospun PLGA-chitosan/PVA membranes and their cytocompatibility in vitro.* Journal of Biomaterials Science, Polymer Edition, 2007. **18**(1): p. 95-115.

30. Qin, Y., *Alginate fibers: an overview of the production processes and applications in wound management.* Polymer International, 2008. **57**(2): p. 171-180.

31. Draget, K., G. Skjåk-Bræk, and O. Smidsrød, *Alginate based new materials.* International Journal of Biological Macromolecules, 1997. **21**(1-2): p. 47-55.

32. Chan, A., R. Whitney, and R. Neufeld, *Kinetic Controlled Synthesis of pH-Responsive Network Alginate.* Biomacromolecules, 2008.

33. Khromova, Y.L., *The effect of chlorides on alginate gelation in the presence of calcium sulfate.* Colloid Journal, 2006. **68**(1): p. 115-119.

34. Kuo, C. and P. Ma, *Ionically crosslinked alginate hydrogels as scaffolds for tissue engineering: Part 1. Structure, gelation rate and mechanical properties.* Biomaterials, 2001. **22**(6): p. 511-521.

35. Said, A.A., M.M.M. Abd El-Wahab, and R.M. Hassan, *Thermal and electrical studies on some metal alginate compounds.* Thermochimica Acta, 1994. **233**(1): p. 13-24.

36. Cathell, M., *Structurally colored biopolymer thin films for detection of dissolved metal ions in aqueous solution*, in *Materials Science and Engineering*. 2008, Drexel University.

37. Cathell, M.D. and C.L. Schauer, *Structurally Colored Thin Films of Ca2+-Cross-Linked Alginate.* Biomacromolecules, 2007. **8**(1): p. 33-41.

38. Gombotz, W. and S. Wee, *Protein release from alginate matrices.* Advanced Drug Delivery Reviews, 1998. **31**(3): p. 267-285.

39. Yuk, S.H., S.H. Cho, and H.B. Lee, *pH-sensitive drug delivery system using O/W emulsion.* Journal of Controlled Release, 1995. **37**(1-2): p. 69-74.

40. HARI, P., *Chitosan/Calcium-Alginate Beads for Oral Delivery of Insulin.* Journal of Applied Polymer Science, 1996. **59**: p. 1795-1801.

41. Hashimoto, T., et al., *Review Peripheral nerve regeneration using non-tubular alginate gel crosslinked with covalent bonds.* Journal of Materials Science Materials in Medicine, 2005. **16**(6): p. 503-509.

42. Laurent, T. and J. Fraser, *Hyaluronan.* FASEB J, 1992. **6**(7): p. 2397-404.

43. Tomihata, K. and Y. Ikada, *Crosslinking of hyaluronic acid with water-soluble carbodiimide.* Journal of biomedical materials research, 1997. **37**(2): p. 243-51.

44. Tomihata, K. and Y. Ikada, *Crosslinking of hyaluronic acid with glutaraldehyde.* Journal of Polymer Science Part A Polymer Chemistry, 1997. **35**(16): p. 3553-3559.

45. Collins, M. and C. Birkinshaw, *Physical properties of crosslinked hyaluronic acid hydrogels.* J Mater Sci Mater Med, 2008.

46. Collins, M. and C. Birkinshaw, *Comparison of the effectiveness of four different crosslinking agents with hyaluronic acid hydrogel films for tissue-culture applications.* Journal of Applied Polymer Science, 2007. **104**(5): p. 3183-3191.

47. Ramamurthi, A. and I. Vesely, *Evaluation of the matrix-synthesis potential of crosslinked hyaluronan gels for tissue engineering of aortic heart valves.* Biomaterials, 2005. **26**(9): p. 999-1010.

48. Huskisson, E., *Hyaluronic acid in the treatment of osteoarthritis of the knee*. 1999, Br Soc Rheumatology. p. 602-607.

49. Ji, Y., et al., *Electrospun three-dimensional hyaluronic acid nanofibrous scaffolds.* Biomaterials, 2006. **27**(20): p. 3782-3792.

50. Kim, T., H. Chung, and T. Park, *Macroporous and nanofibrous hyaluronic acid/collagen hybrid scaffold fabricated by concurrent electrospinning and deposition/leaching of salt particles.* Acta Biomaterialia, 2008.

51. Yoo, H., et al., *Hyaluronic acid modified biodegradable scaffolds for cartilage tissue engineering.* Biomaterials, 2005. **26**(14): p. 1925-1933.

52. Solchaga, L., et al., *Hyaluronic acid-based polymers as cell carriers for tissue-engineered repair of bone and cartilage.* Journal of Orthopaedic Research, 1999. **17**(2): p. 205-213.

53. Huang, Z., et al., *A review on polymer nanofibers by electrospinning and their applications in nanocomposites.* Composites Science and Technology, 2003. **63**(15): p. 2223-2253.

54. D. Li, Y.X., *Electrospinning of Nanofibers: Reinventing the Wheel?* Advanced Materials, 2004. **16**(14): p. 1151-1170.

55. Doshi, J. and D.H. Reneker. *Electrospinning process and applications of electrospun fibers*. in *Industry Applications Society Annual Meeting, 1993., Conference Record of the 1993 IEEE*. 1993.

56. Young, D., *Hyaluronic Acid-based Nanofibers via Electrospinning.* 2006.
57. Yarin, A., S. Koombhongse, and D. Reneker, *Taylor cone and jetting from liquid droplets in electrospinning of nanofibers.* Journal of Applied Physics, 2001. **90**: p. 4836.

58. Cloupeau, M. and B. Prunet-Foch, *Electrostatic spraying of liquids: main functioning modes.* J. Electrostatics, 1990. **25**(2): p. 165-184.

59. Reneker, D., et al., *Bending instability of electrically charged liquid jets of polymer solutions in electrospinning.* Journal of Applied Physics, 2000. **87**: p. 4531.

60. Subbiah, T., et al., *Electrospinning of nanofibers.* Journal of Applied Polymer Science, 2005. **96**(2): p. 557-569.

61. Frenot, A. and I. Chronakis, *Polymer nanofibers assembled by electrospinning.* Current Opinion in Colloid & Interface Science, 2003. **8**(1): p. 64-75.

62. Zong, X., et al., *Structure and process relationship of electrospun bioabsorbable nanofiber membranes.* Polymer, 2002. **43**(16): p. 4403-4412.

63. Lam, H., *Electrospinning of single wall carbon nanotube reinforced aligned fibrils and yarns*. 2004, Drexel University.

64. Berry, G.C., *Thermodynamic and Conformational Properties of Polystyrene. II. Intrinsic Viscosity Studies on Dilute Solutions of Linear Polystyrenes.* The Journal of Chemical Physics, 1967. **46**(4): p. 1338-1352.

65. Ali, A., *Carbon nanotube reinforced carbon nano composite fibrils by electro-spinning*. 2003, Drexel University.

66. Ko, F., *Nanofiber Technology.* Nanotubes and Nanofibers, 2006.

67. Thompson, C., et al., *Effects of parameters on nanofiber diameter determined from electrospinning model.* Polymer, 2007. **48**(23): p. 6913-6922.

68. PAINTER, P. and M. COLEMAN, *FUNDAMENTALS OF POLYMER SCIENCE: AN INTRODUCTORY TEXT*. 1997: Technomic Publishing Co., Inc.

69. Yu, J., S. Fridrikh, and G. Rutledge, *The role of elasticity in the formation of electrospun fibers.* Polymer, 2006. **47**(13): p. 4789-4797.

70. Theron, S., E. Zussman, and A. Yarin, *Experimental investigation of the governing parameters in the electrospinning of polymer solutions.* Polymer, 2004. **45**(6): p. 2017-2030.

71. Kim, S., C. Lee, and S. Kim, *Effect of ionic salts on the processing of poly (2-acrylamido-2-methyl-1-propane sulfonic acid) nanofibers.* Journal of Applied Polymer Science, 2005. **96**(4): p. 1388-1393.

72. Lu, J.-W., et al., *Electrospinning of sodium alginate with poly(ethylene oxide).* Polymer, 2006. **47**(23): p. 8026-8031.

73. Deitzel, J., et al., *The effect of processing variables on the morphology of electrospun nanofibers and textiles.* Polymer, 2001. **42**(1): p. 261-272.

74. Demir, M., et al., *Electrospinning of polyurethane fibers.* Polymer, 2002. **43**(11): p. 3303-3309.

75. Yuan, X., et al., *Morphology of ultrafine polysulfone fibers prepared by electrospinning.* Polymer International, 2004. **53**(11): p. 1704-1710.

76. Li, D. and Y. Xia, *Direct Fabrication of Composite and Ceramic Hollow Nanofibers by Electrospinning.* Nano Lett., 2004. **4**(5): p. 933-938.

77. Deitzel, J.M., et al., *Controlled deposition of electrospun poly(ethylene oxide) fibers.* Polymer, 2001. **42**(19): p. 8163-8170.

78. Casper, C., et al., *Controlling Surface Morphology of Electrospun Polystyrene Fibers: Effect of Humidity and Molecular Weight in the Electrospinning Process.* Macromolecules, 2004. **37**(2): p. 573-578.

79. Bhattarai, N. and M. Zhang, *Controlled synthesis and structural stability of alginate-based nanofibers.* Nanotechnology, 2007. **18**(45): p. 455601.

80. Lee, Y.J., et al., *Preparation of atactic poly(vinyl alcohol)/sodium alginate blend nanowebs by electrospinning.* Journal of Applied Polymer Science, 2007. **106**(2): p. 1337-1342.

81. Safi, S., et al., *Study of electrospinning of sodium alginate, blended solutions of sodium alginate/poly (vinyl alcohol) and sodium alginate/poly (ethylene oxide).* Journal of Applied Polymer Science, 2007. **104**(5): p. 3245-3255.

82. Nie, H., et al., *Effects of Chain Conformation and Entanglement on the Electrospinning of Pure Alginate.* Biomacromolecules, 2008. **9**(5): p. 1362-1365.

83. Li, J., et al., *Electrospinning of Hyaluronic Acid (HA) and HA/Gelatin Blends.* MACROMOLECULAR RAPID COMMUNICATIONS, 2006. **27**(2): p. 114.

84. Um, I., et al., *Electro-Spinning and Electro-Blowing of Hyaluronic Acid.* BIOMACROMOLECULES-WASHINGTON-, 2004. **5**(4): p. 1428-1436.

85. Chen, H., J. Snyder, and Y. Elabd, *Electrospinning and Solution Properties of Nafion and Poly (acrylic acid).* Macromolecules, 2008. **41**(1): p. 128-135.

86. Ding, B., M. Yamazaki, and S. Shiratori, *Electrospun fibrous polyacrylic acid membrane-based gas sensors.* Sensors & Actuators: B. Chemical, 2005. **106**(1): p. 477-483.

87. Li, L. and Y. Hsieh, *Ultra-fine polyelectrolyte fibers from electrospinning of poly (acrylic acid).* Polymer, 2005. **46**(14): p. 5133-5139.

88. Okubo, T., *Extraordinary properties of synthetic and biological polyelectrolytes in deionized solution. 1. Extended conformation of poly (acrylic acid).* J. Phys. Chem, 1989. **93**(18): p. 6860-6863.

89. Maleki, A., A. Kjoniksen, and B. Nystrom. *Effect of pH on the Behavior of Hyaluronic Acid in Dilute and Semidilute Aqueous Solutions*. 2008: WILEY-VCH Verlag Weinheim.

90. Tokita, Y. and A. Okamoto, *Hydrolytic degradation of hyaluronic acid.* Polymer Degradation and Stability, 1995. **48**(2): p. 269-273.

91. Bhumkar, D. and V. Pokharkar, *Studies on effect of pH on cross-linking of chitosan with sodium tripolyphosphate: A technical note.* AAPS PharmSciTech, 2006. **7**(2): p. 138-143.

92. Shu, X. and K. Zhu, *The influence of multivalent phosphate structure on the properties of ionically cross-linked chitosan films for controlled drug release.* European Journal of Pharmaceutics and Biopharmaceutics, 2002. **54**(2): p. 235-243.

93. Rayment, P. and M. Butler, *Investigation of ionically crosslinked chitosan and chitosan-bovine serum albumin beads for novel gastrointestinal functionality.* Journal of Applied Polymer Science, 2008. **108**(5).

94. Chenite, A., et al., *Rheological characterisation of thermogelling chitosan/glycerol-phosphate solutions.* Carbohydrate Polymers, 2001. **46**(1): p. 39-47.

95. Chenite, A., et al., *Novel injectable neutral solutions of chitosan form biodegradable gels in situ.* Biomaterials, 2000. **21**(21): p. 2155-2161.

96. Koombhongse, S., W. Liu, and D. Reneker, *Flat polymer ribbons and other shapes by electrospinning.* Journal of Polymer Science Part B: Polymer Physics, 2001. **39**(21): p. 2598-2606.

97. Spasova, M., et al., *Perspectives On: Criteria for Complex Evaluation of the Morphology and Alignment of Electrospun Polymer Nanofibers.* Journal of Bioactive and Compatible Polymers, 2006. **21**(5): p. 465.

98. Wu, X. and Y. Dzenis, *Collapse analysis of nanofibres.* Nanotechnology, 2007. **18**(28): p. 285702-285702.

99. Manku, G. and M. Staff, *Theoretical principles of inorganic chemistry*. 1980: Tata McGraw-Hill.

100. McKee, M., et al., *Correlations of Solution Rheology with Electrospun Fiber Formation of Linear and Branched Polyesters.* Macromolecules, 2004. **37**(5): p. 1760-1767.

101. Klossner, R., et al., *Correlation of Chitosan's Rheological Properties and Its Ability to Electrospin.* Biomacromolecules, 2008.

102. Schiffman, J.D., *Determination of the electrospinning parameters for electrospinning of biopolyelectrolytes and their modifications*, in *Materials Science and Engineering*. 2009, Drexel University: Philadelphia.

CHAPTER 8

Appendix A: Chemicals and Reagents

Chemical	Molecular Weight	Manufacturer	Grade
Sodium alginate (Na Salt)	80-120K	Sigma-Aldrich	M/G: 1.56
Hyaluronic acid (Na Salt)	$2.12x10^6$	Avon	Cosmetic
Hyaluronic acid (Na Salt)	$2.0x10^6$	Dali Chemical Co. (Liuzhou, China)	Cosmetic
HMW chitosan	500-700K	Sigma-Aldrich	DD: 72
MMW chitosan	190-310K	Sigma-Aldrich	DD: 83
LMW chitosan	70K	Sigma-Aldrich	DD: 74
PG chitosan	190-375K	Sigma-Aldrich	DD: 75
Poly (ethylene oxide)	600K	Sigma-Aldrich	-
Glycerol	N/A	Sigma-Aldrich	≥99%
Acetic acid	N/A	Sigma-Aldrich	99.7% ACS Reagent
Trifluoroacetic acid (TFA)	N/A	Sigma-Aldrich	99% Reagent +
Sodium hydroxide	N/A	Sigma-Aldrich	97% ACS Reagent
Dimethylformamide (DMF)	N/A	Sigma-Aldrich	99.8% ACS Reagent
Isopropyl alcohol	N/A	Sigma-Aldrich	≥99%
Acetone	N/A	Sigma-Aldrich	99.50%
Methanol	N/A	VWR International	99.8% ACS Reagent
Gutaraldehyde	N/A	Sigma-Aldrich	50% in Water
Divinyl sulfone	N/A	Sigma-Aldrich	97%
Deionized Water	N/A	Millipore Milli-Q Plus filtration system	-
Ethanol	N/A	Decon Labs Inc	200 proof
Sodium phosphate	N/A	Fluka	≥99%
Ammonium hydroxide	N/A	Fluka	25% in Water
Sodium tripolyphosphate	N/A	Sigma-Aldrich	85%
Glycerol phosphate	N/A	Sigma-Aldrich	disodium salt hydrate
Phosphate buffered saline	N/A	Sigma-Aldrich	pH 7.4, 10mM

Appendix B: Alginate Electrospinning Trials

Polymer 1	Alginate	Alginate	Alginate	Alginate	Alginate	Alginate	Alginate	Alginate	Alginate	Alginate	Alginate	Alginate	Alginate	Alginate	Alginate	Alginate	Alginate	Alginate	Alginate	Alginate	Alginate	Alginate	Alginate	Alginate	Alginate	Alginate	Alginate	Alginate	Alginate	Alginate
Polymer 2	PEO	PEO	PEO	PEO	PLA	PLA	PEO	PEO	Alginate	PEO	PEO	PEO	Alginate	Alginate	Alginate	Alginate	Alginate	Alginate	Alginate	Alginate	Alginate	Alginate	Alginate	Alginate	Alginate	Alginate	Alginate	Alginate	Alginate	Alginate
Salt (s)	N/A	N/A	N/A	N/A	N/A	N/A	N/A	N/A	N/A	N/A	N/A	N/A	N/A	N/A	N/A	N/A	N/A	N/A	N/A	N/A	N/A	N/A	N/A	N/A	N/A	N/A	N/A	N/A	N/A	N/A
Wt Polymer 1 (g)	0.05	0.075	0.1	0.15	0.15	0.3	0.6	0.45	0.4	0.2	0.15	0.3	0.3	0.3	0.32	0.375	0.45	0.3	0.3	0.45	0.225	0.45	0.45	0.3	0.6	0.45	0.45	0.3	0.28	
Wt Polymer 2 or Salt (g)	0.05	0.075	0.1	0.15	0.15	3	0	0.15	0.2	0.4	0.45	0.6	0.3	0.3	0.32	0.375	0.45	0.3	0.3	0.45	0.225	0.45	0.225	0.15	0.3	0.45	0.45	0.3	0.28	
Polymer1: Polymer2 Ratio (wt)	1:1	1:1	1:1	1:1	1:1	1:1	1:0	3:1	2:1	1:2	1:3	0:1	N/A	N/A	N/A	N/A	N/A	N/A	N/A	N/A	N/A	N/A	2:1	2:1	2:1	N/A	N/A	N/A	N/A	N/A
Crosslinker	N/A	N/A	N/A	N/A	N/A	N/A	N/A	N/A	N/A	N/A	N/A	N/A	N/A	N/A	N/A	N/A	N/A	N/A	N/A	N/A	N/A	N/A	N/A	N/A	N/A	N/A	N/A	N/A	N/A	N/A
Vol Crosslinker (ml)	N/A	N/A	N/A	N/A	N/A	N/A	N/A	N/A	N/A	N/A	N/A	N/A	N/A	N/A	N/A	N/A	N/A	N/A	N/A	N/A	N/A	N/A	N/A	N/A	N/A	N/A	N/A	N/A	N/A	N/A
Wt. Crosslinker (g)	N/A	N/A	N/A	N/A	N/A	N/A	N/A	N/A	N/A	N/A	N/A	N/A	N/A	N/A	N/A	N/A	N/A	N/A	N/A	N/A	N/A	N/A	N/A	N/A	N/A	N/A	N/A	N/A	N/A	N/A
Solvent(s)	H2O	H2O	H2O	H2O	H2O	H2O	H2O	H2O	H2O	H2O	H2O	H2O	H2O/ Glycerol	H2O/ Glycerol	H2O/ Glycerol	H2O/ Glycerol	H2O/ Glycerol	Isopropyl alcohol/ Glycerol	Isopropyl alcohol/ Glycerol	Isopropyl alcohol/ acetone	H2O/ acetone	DMF: H2O	DMF: H2O	1% Acetic Acid	Aqueous NaOH	Aqueous NaOH	.5M NaOH/ Methanol	.5M NaOH/ Methanol	.5M NaOH/ DMF	.5M NaOH/ DMF
Vol. Solvents (mL)	10	10	10	10	10	20	20	20	20	20	20	20	5/10	1/14	7.5/7.5	4/12	5/10	5/10	12/2	7/7	4/10	6/9	9/6	9/6	15	15	15	12/3	3/12	12/3	12/2
Concentration (w/v %)	1	1.5	2	3	3	3	3	3	3	3	3	3	2	2	2	2	2.5	3	2.14	2.14	2.14	2	3	1.5	3	3	2	4	3	3	2	2
Spinnable?			Yes	Yes	No	No	No	Maybe	Yes	Yes	Yes	Yes	Maybe	Maybe	Maybe	Maybe	Maybe	No	No	No	No	No	No	No	Maybe	No	Maybe	No	No	No	No
Temp (°F)			73	75				72	72	72	72	72	72	75	73	72								74	70		71				
Humidity (%)			32	29				34	34	34	34	34	32	31	29	55								51	28		30				
Voltage (KV)			15	18				18	17	17	17	17	20-25	20-25	20-22	23								Tried All	Tried All	Tried All	Tried All				
Speed			1 mL/hr	0.8, 1.0 mL/hr				0.7 mL/hr	0.7 mL/hr	0.7 mL/hr	0.7 mL/hr	0.7 mL/hr	.006-1.0 mL/hr	.5-1.0 mL/hr	0.5 mL/hr	1.3 mL/hr								Tried All	Tried All	Tried All	Tried All				
Target Distance (cm)			9	10cm				5	6	6	6	6	7-13	7-10	7	5-6								Tried All							

Appendix C: Hyaluronic Acid Electrospinning Trials

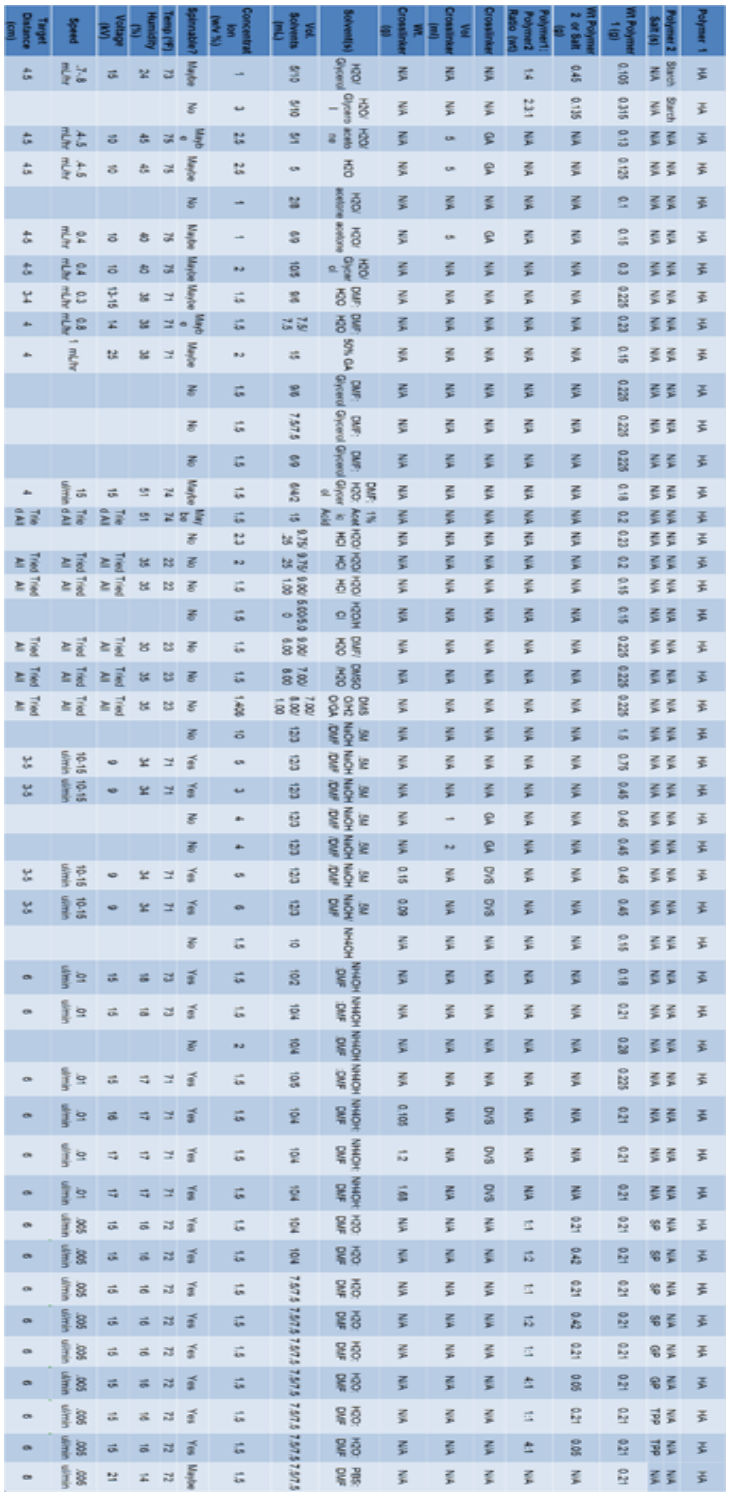

Appendix D:

FTIR of HA electrospinning solutions in NaOH:DMF after various mixing times

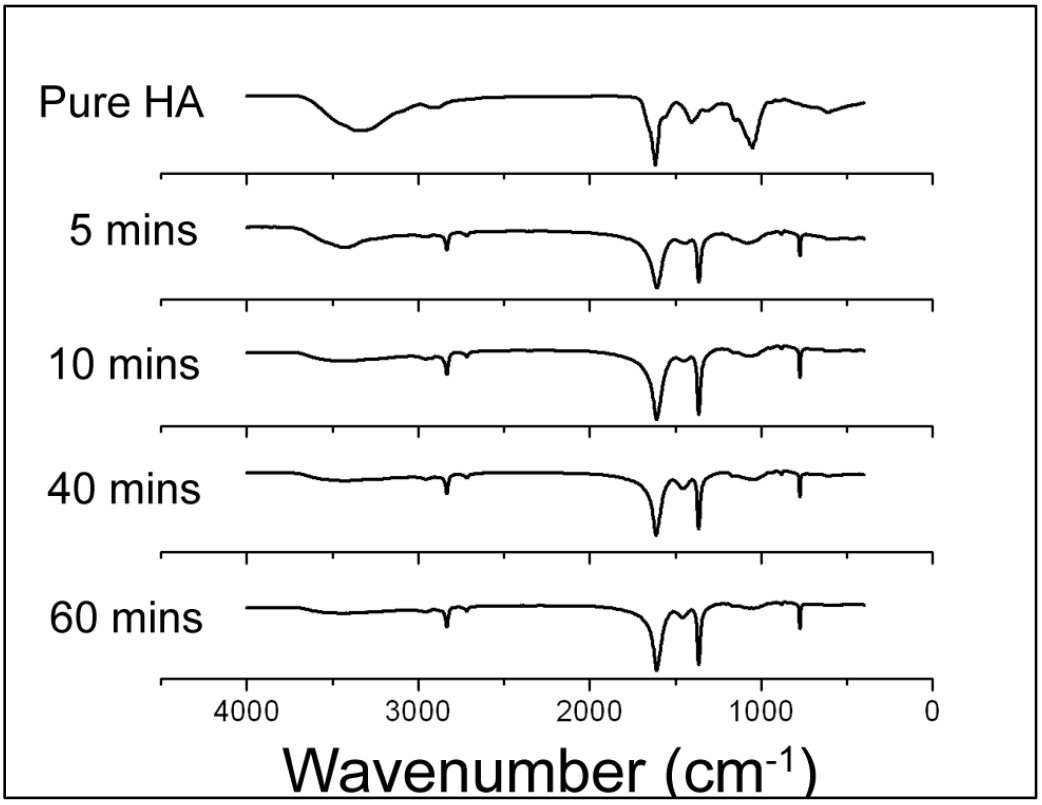

Appendix E:

FTIR spectra for SP, GP and TPP salts in comparison with HA fibers

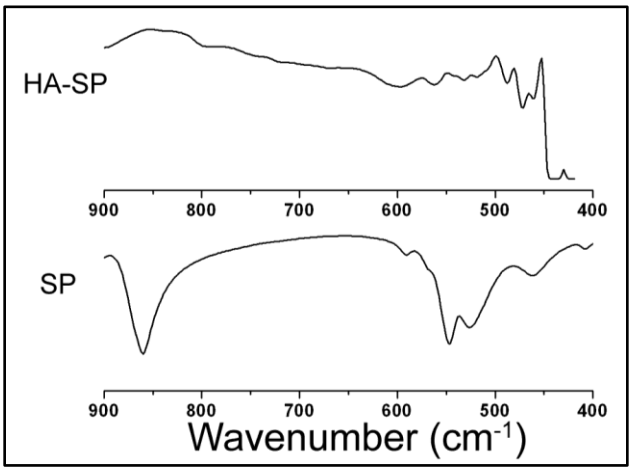

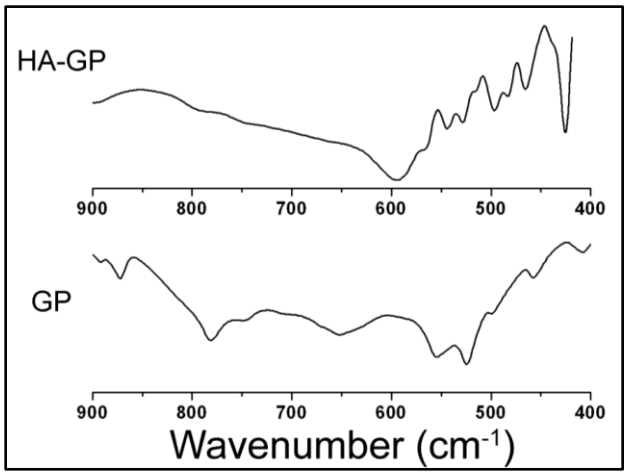

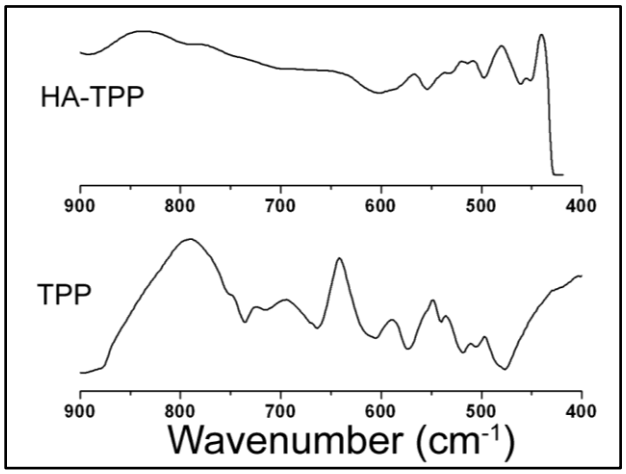

Appendix F:

Apparent viscosity versus shear rate for phosphate containing solutions

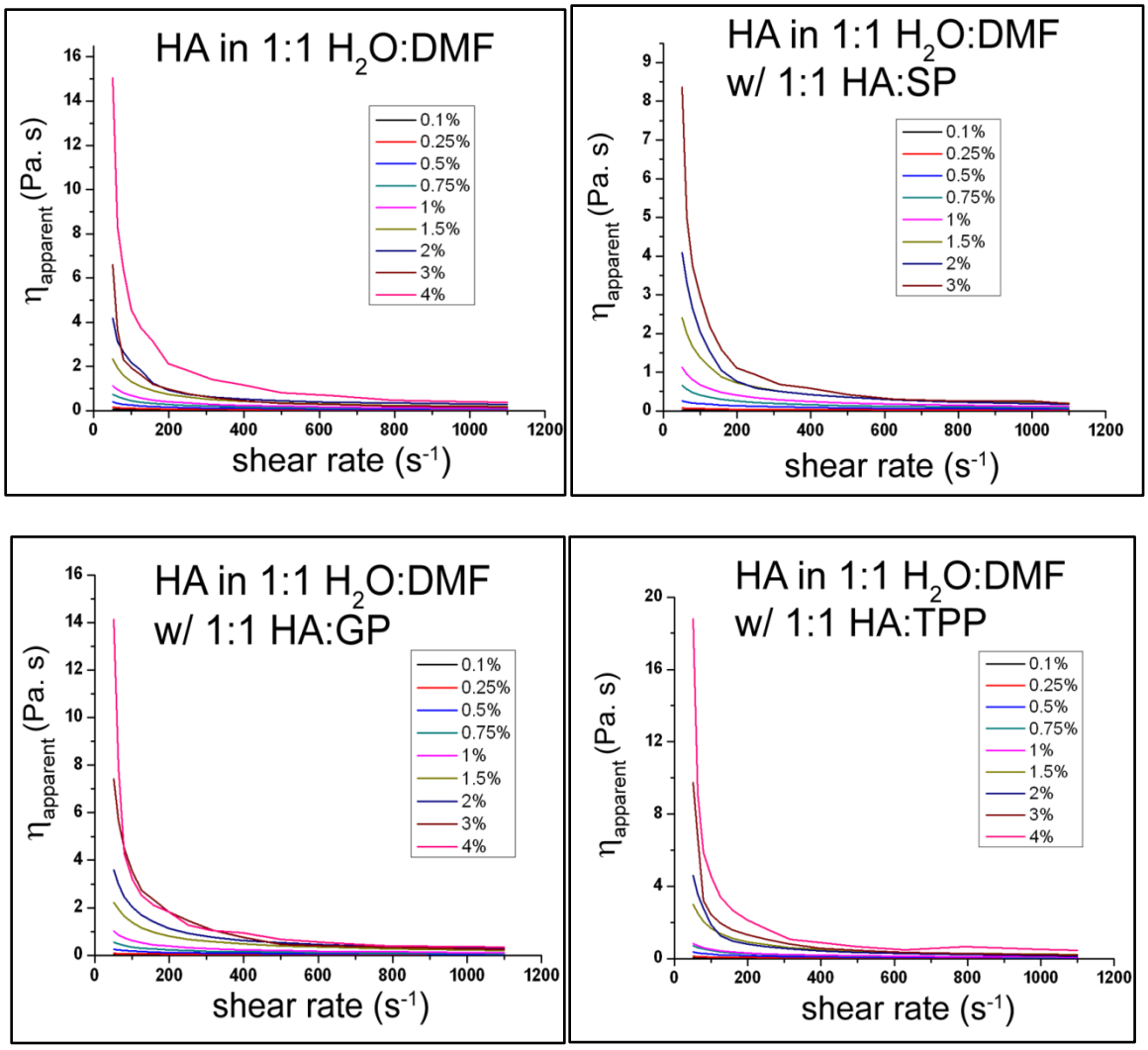

Appendix G:

Specific viscosity versus shear rate for phosphate containing solutions